

Methyl Transfer Reactivity of Five-Coordinate $\text{CH}_3\text{Co}^{\text{III}}\text{Pc}$

Włodzimierz Galezowski*

Department of Chemistry, A. Mickiewicz University, Grunwaldzka 6, 60-780 Poznan, Poland

Received September 16, 2004

$\text{CH}_3\text{Co}^{\text{III}}\text{Pc}$ (Pc = dianion of phthalocyanine) has been characterized by equilibrium studies of its trans axial ligation and cyclic voltammetry as a relatively “electron poor” model of methylcobalamin, which in noncoordinating solvents persists as a five-coordinate complex. Axial base (N-donors, PBu_3 , SCN^- , weakly binding O-donors) inhibition of methyl transfer from $\text{CH}_3\text{Co}^{\text{III}}\text{Pc}$ shows that the reaction proceeds via the reactive five-coordinate species, even in coordinating solvents. The virtual inactivity of six-coordinate $\text{CH}_3\text{Co}^{\text{III}}\text{Pc}(\text{L})$ complexes provides a reference point for important biological processes.

Introduction

Methylcobalamin, MeCbl ,¹ is an intermediate in biologically important processes. Both methyl transfer to cob(I)-alamin and demethylation of the resulting MeCbl are generally believed to proceed by an $\text{S}_{\text{N}}2$ mechanism, although oxidative addition and electron transfer mechanism have been recently considered.² Nonenzymatic methyl transfer from MeCbl , and other methylcorrinoids, even to excellent nucleophiles such as thiolates,^{3,4,5} proceeds sluggishly. It is no wonder that there have been very few reports of MeCbl models that transfer CH_3^+ at a reasonable rate.⁶ A suitable methylcobalt(III) model has to be more reactive than MeCbl . Methylcobinamide (MeCbi^+), lacking the dimethylbenzimidazole nucleotide tail, which in MeCbl is usually coordinated to cobalt, reacts with homocysteine at least 1500-fold faster than MeCbl .⁵ However, that is in comparison to the unmeasurably slow reaction of MeCbl at 25 °C. In early works

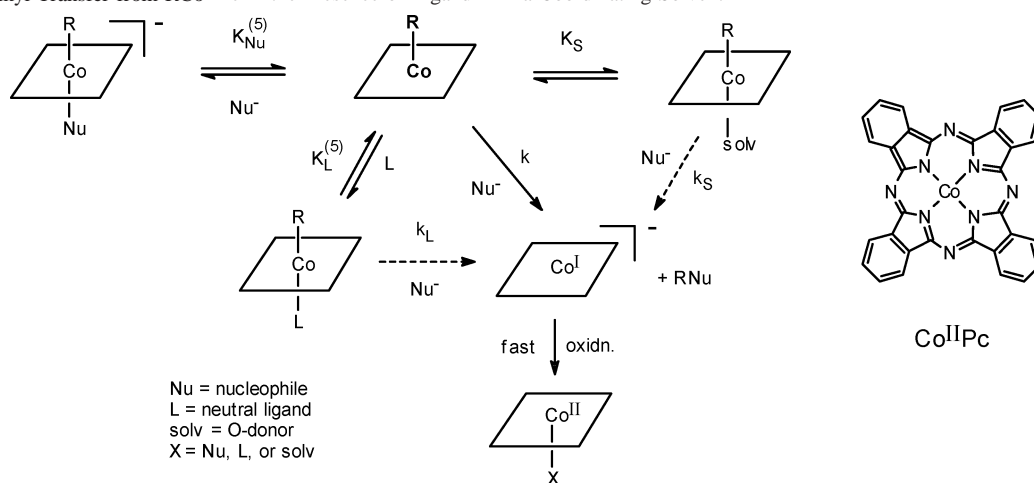
of Schrauzer et al., an activated methylcobaloxime, $\text{CH}_3\text{Co}(\text{DBF}_2)_2$ ⁷ has been found to react rapidly with phosphines⁷ and slowly with thiolates.⁸ With ordinary nucleophiles: halides, thiocyanate, cyanide, or selenides, alkylcobaloximes either do not react or react only under drastic conditions with poor yields, not allowing a detailed kinetic study.^{7–9}

In our earlier work, methylcobalt(III) phthalocyanine ($\text{CH}_3\text{Co}^{\text{III}}\text{Pc}$) was shown to transfer CH_3^+ to nucleophiles that are unable to attack MeCbl or MeCbi^+ such as iodide, bromide, and cyanide¹⁰ and, in a rapid process, to thiophenoxide¹¹ by an $\text{S}_{\text{N}}2$ mechanism. In view of the scarcity of data on methyl transfer from cobalt, further studies involving a broader range of nucleophiles seem warranted. The enhanced reactivity stems in part from 3 to 5 orders of magnitude faster methyl transfer rates in aprotic solvents, in which $\text{RCo}^{\text{III}}\text{Pc}$ complexes are soluble, than in aqueous solution.¹² The demethylation is also relatively fast because $\text{Co}^{\text{I}}\text{Pc}^-$ being one of the weakest cobalt supernucleophiles known, both kinetically¹³ and thermodynamically,¹⁰ is a good leaving group.¹⁰ High reactivity of $\text{CH}_3\text{Co}^{\text{III}}\text{Pc}$ can also be explained differently: Identity methyl transfer between two $\text{Co}^{\text{I}}\text{Pc}^-$ nucleophiles estimated from the Marcus cross-relation is rapid (11.8 and 51 $\text{M}^{-1} \text{s}^{-1}$ in dimethylacetamide¹⁰ and sulfolane,¹⁴ respectively), and the demethylation reactions

* E-mail: wlodgal@amu.edu.pl.

- (1) Abbreviations: Pc, dianion of phthalocyanine; Cbi⁺, cobinamide; Cbl, cobalamin; OEP, dianion of 2,3,7,8,12,13,17,18-octaethylporphyrin; TPP, dianion of 5,10,15,20-tetraphenylporphyrin; DH, monoanion of dimethylglyoxime; (DO)(DOH)pn, anion of $N^2, N^{2'}$ -propanediylbis(2,3-butanedione 2-imine-3-oxime); salen, dianion of bis(salicydene)-ethylenediamine; saloph, dianion of bis(salicylidene)-*o*-phenylenediamine; bae, dianion of bis(acetylacetonate)ethylenediamine; py, pyridine; N-MeIm, *N*-methylimidazole; DMA, dimethylacetamide; DMF, dimethylformamide; DMSO, dimethyl sulfoxide; DABCO, 1,4-diazabicyclo-[2.2.2]octane.
- (2) Matthews, R. G. *Acc. Chem. Res.* **2001**, *34*, 681.
- (3) Hogenkamp, H. P. C.; Bratt, G. T.; Dun, S.-Z. *Biochemistry* **1985**, *24*, 6428.
- (4) Hogenkamp, H. P. C.; Bratt, G. T.; Kotchevar, A. T. *Biochemistry* **1987**, *26*, 4723.
- (5) Norris, P. R.; Pratt, J. M. *BioFactors* **1996**, *5*, 240.
- (6) (a) Brown, K. L.; Brooks, H. B. *Inorg. Chem.* **1991**, *30*, 3420 and references therein. (b) Toscano, P. J.; Marzilli, L. G. *Prog. Inorg. Chem.* **1984**, *31*, 105.

- (7) Stadlauber, E. A.; Holland, R. J.; Lamm, F. P.; Schrauzer, G. N. *Bioinorg. Chem.* **1974**, *4*, 67 and references therein.
- (8) Schrauzer, G. N.; Stadlauber, E. A. *Bioinorg. Chem.* **1974**, *3*, 353.
- (9) Schrauzer, G. N. *Acc. Chem. Res.* **1968**, *1*, 97.
- (10) Galezowski, W.; Ibrahim, P. N.; Lewis, E. S. *J. Am. Chem. Soc.* **1993**, *115*, 8660.
- (11) Galezowski, W.; Lewis, E. S. *J. Org. Phys. Chem.* **1994**, *7*, 90.
- (12) However, aprotic medium may mimic hydrophobic conditions in the active site of a methyltransferase and, in particular, larger than in water nucleophilic strength of the methyl acceptor.
- (13) Eckert, H. E.; Ugi, I. *Angew. Chem.* **1975**, *87*, 826.

Scheme 1. Alkyl Transfer from $\text{RCo}^{\text{III}}\text{Pc}$ in the Presence of Ligand L in a Coordinating Solvent

of $\text{CH}_3\text{Co}^{\text{III}}\text{Pc}$ are not as much uphill as with MeCbl and most of its models.

Axial base effect on the rate of methyl transfer has not been studied as extensively as in the case of homolytic cleavage of the $\text{Co}-\text{C}$ bond,¹⁵ but recently there has been a growing interest in it. Simple considerations supported by theoretical studies¹⁶ lead to a conclusion that the axial base should deactivate $\text{R}(\text{Co}^{\text{III}})$ species against nucleophilic attack at $\text{Co}-\text{C}$ bond by increasing electron density on the carbon atom. Relevant experimental findings are confined to corrinoid, mostly enzymatic, chemistry.^{17,18} A physiological methyl donor, the methyl-cobalt(III) state of corrinoid iron-sulfur protein of *Moorella thermoacetica*, exists in five-coordinate form.¹⁹ However, in methionine synthase, probably the most studied methyltransferase, the cobalamine is six-coordinate (base-off but "histidine-on").¹⁸ Enhanced methyl transfer rates, typically 3 orders of magnitude, have been observed on replacement of MeCbl with MeCbi^+ .^{20,21} Occasionally exogenous N-donor inhibition of enzymatic methyl transfer involving MeCbi^+ has also been studied. In one case the inhibition could not be accounted for by the equilibrium constant of ligand association by cobalt.²² In another it was consistent with the equilibrium constant, while unexpected pyridine inhibition of the MeCbl reaction occurred, which was explained by "organic solvent effect" on the protein.²³ (Because of small association constants of N-donors such as pyridine or imidazole with MeCbi^+ these inhibition studies require high N-donor concentrations in

aqueous solution.) The effect of trans axial ligation on heterolytic methyl transfer from cobalt is relevant to biological systems and it seems worthwhile studying with a simple nonenzymatic model.

In our earlier work, the effect of neutral axial bases on $\text{S}_{\text{N}}2$ reactivity of $\text{CH}_3\text{Co}^{\text{III}}\text{Pc}$ has not been explored, but it has been noted that when an anionic nucleophile ($\text{Nu} = \text{CN}^-$, PhS^-) ligates the substrate (Scheme 1) a kinetic saturation of methyl transfer is observed,^{10,11} which was explained by inertness of the negatively charged $\text{CH}_3\text{Co}^{\text{III}}\text{Pc}(\text{Nu})^-$ adducts. This work will show that such atypical, for an $\text{S}_{\text{N}}2$ reaction, concentration dependencies of the rates are observed with variety of other, not only anionic, nucleophiles.

The fact that demethylations of $\text{CH}_3\text{Co}^{\text{III}}\text{Pc}$ are most conveniently studied in polar aprotic solvents brings up the question of O-donor inhibition. It is of interest to see if kinetic competence of the five-coordinate species in the presence of weak binding O-donors can be demonstrated. Five-coordinate alkylcobalt(III) complexes have been known for decades although their existence in solution has also been contested.²⁴ Early Pratt and co-workers' studies of temperature-induced changes in the visible spectra of alkylcobinamides in aqueous solution,²⁵ and also recent reports on pressure effects on the spectra and the rates of ligand exchange,^{26,27} demonstrate that RCbi^+ should be regarded as five-coordinate complexes in rapid equilibrium with six-coordinate aqua complexes.

This work focuses on reactive forms of the organocobalt(III) substrate. In Scheme 1, $\text{RCo}^{\text{III}}\text{Pc}$ dissolved in a coordinating solvent in the presence of a neutral axial base, L, that is unable to attack the $\text{Co}-\text{C}$ bond, transfers its primary alkyl group, R, to a nucleophile, Nu^- ,²⁸ that also shows an ability to ligate the substrate. The methyl transfer

- (14) Galezowski, W. *Pol. J. Chem.* **2001**, *75*, 949.
 (15) (a) Jensen, M. P.; Halpern, J. *J. Am. Chem. Soc.* **1999**, *121*, 2181. (b) Sirovatka, J. M.; Finke, R. G. *Inorg. Chem.* **1999**, *38*, 1697. (c) Brown, K. L.; Marques, H. M. *J. Inorg. Biochem.* **2001**, *83*, 121. (d) Jensen, K. P.; Ryde, U. *J. Mol. Struct.* **2002**, *585*, 239 and references therein.
 (16) Dölker, N.; Maseras, F.; Lledós, A. J. *Phys. Chem. B* **2003**, *107*, 306.
 (17) Kräutler, B. *Helv. Chim. Acta* **1987**, *70*, 1268.
 (18) Drennan, C. L.; Huang, S.; Drummond, J. T.; Matthews, R. G.; Ludwig, M. L. *Science* **1994**, *266*, 1669.
 (19) Wirt, W. D.; Kumar, M.; Wu, J.-J.; Scheuring, E. M.; Ragsdale, S.; Chance, M. *Biochemistry* **1995**, *34*, 5269.
 (20) Seravalli, J.; Brown, K. L.; Ragsdale, S. W. *J. Am. Chem. Soc.* **2001**, *123*, 1786.
 (21) Bandarian, V.; Matthews, R. G. *Biochemistry* **2001**, *40*, 5056.
 (22) Sauer, K.; Thauer, R. K. *Eur. J. Biochem.* **1999**, *261*, 674.
 (23) Sirovatka-Dorweiler, J.; Finke, R. G.; Matthews, R. G. *Biochemistry* **2003**, *42*, 14653.

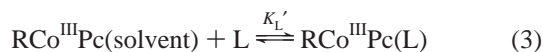
- (24) Sirovatka, J. M.; Finke, R. G. *J. Am. Chem. Soc.* **1997**, *119*, 3057 and references therein.
 (25) Firth, R. A.; Hill, H. A. O.; Mann, B. E.; Pratt, J. M. *J. Chem. Soc. A* **1968**, 2419.
 (26) Hamza, M. S. A.; van Eldik, L. S.; Harper, L. S.; Pratt, J. M.; Betterton, E. A. *Eur. J. Inorg. Chem.* **2002**, 580.
 (27) Hamza, M. S. A.; Zou, X.; Brown, K. L.; van Eldik, R. *Eur. J. Inorg. Chem.* **2003**, 268.
 (28) In Scheme 1 an anionic nucleophile is shown, but it might be neutral as well.

step is pictured as an irreversible reaction because of fast scavenging of the primary product, $\text{Co}^{\text{I}}\text{Pc}^-$, by trace oxidants. This corresponds to dilute $\text{RCo}^{\text{III}}\text{Pc}$ solutions under not strictly anaerobic conditions (see Experimental Section). The final product is usually $\text{Co}^{\text{II}}\text{Pc}(\text{solvent})$, $\text{Co}^{\text{II}}\text{Pc}(\text{L})$, or $\text{Co}^{\text{II}}\text{Pc}(\text{Nu})^-$, but in concentrated $\text{RCo}^{\text{III}}\text{Pc}$ solutions of L or Nu, six-coordinate $\text{Co}^{\text{II}}\text{PcL}_2$ or $\text{Co}^{\text{III}}\text{PcNu}_2^-$ complexes may exist in equilibrium with the pentacoordinate product. In Scheme 1, five-coordinate $\text{RCo}^{\text{III}}\text{Pc}$ is indicated as the reactive alkyl donor, while adducts with nucleophile and complexes with strong neutral ligands L or O-donors (solvent) are shown as dead ends ($k_L, k_S \ll k$). Under pseudo-first-order conditions, rate constant expression corresponding to this assumption, is given in eq 1. In a coordinating solvent, in the absence of

$$k_{\text{obs}} = \frac{k[\text{Nu}]}{1 + K_S[\text{solv}] + K_L^{(5)}[\text{L}] + K_{\text{Nu}}^{(5)}[\text{Nu}]} \quad (1)$$

$$k_2 = \frac{k}{1 + K_S[\text{solv}]} \quad (2)$$

L, the substrate exists predominantly as six-coordinate $\text{RCo}^{\text{III}}\text{Pc}(\text{solvent})$ complex, and $k_2 = k_{\text{obs}}/[\text{Nu}]$ is given by eq 2. (In nondonor solvents, k_2 is equal k). In donor solvents, the formation constants $K_{\text{Nu}}^{(5)}$ and $K_L^{(5)}$ shown in Scheme 1 are not easily accessible. Conditional formation constants are determined instead, such as K_L' for reaction 3 To be precise,



we should note that if a usually small concentration of the five-coordinate form is not neglected (the substrate exists in two forms, $\text{RCo}^{\text{III}}\text{Pc}$ and $\text{RCo}^{\text{III}}\text{Pc}(\text{solvent})$), the following expression for practical conditional stability constant, K_L , is obtained

$$K_L = \frac{K_L^{(5)}}{1 + K_S[\text{solv}]} \quad (4)$$

In nondonor solvents, $K_L = K_L^{(5)}$, thus the designation $K_L^{(5)}$ will be used only when coordination of donor solvent to the five-coordinate $\text{RCo}^{\text{III}}\text{Pc}$ species is discussed. By combining eqs 1, 2, and 4, a rate constant expression for methyl transfer reaction in donor solvents is derived:

$$k_{\text{obs}} = \frac{k_2[\text{Nu}]}{1 + K_L[\text{L}] + K_{\text{Nu}}[\text{Nu}]} \quad (5)$$

Kinetic expressions for methyl transfer in donor solvent (eq 5) and nondonor solvent (eq 1, $K_S = 0$) have analogous forms; only definitions of the second-order rate constant and stability constants are different.

Since knowledge of concentrations of different forms in which $\text{CH}_3\text{Co}^{\text{III}}\text{Pc}$ may exist in solution is crucial for estimation of their reactivity, an important part of this work has been measuring formation constants for $\text{RCo}^{\text{III}}\text{Pc}(\text{L})$ complexes.

Although methyl transfer is the main scope of this work, $\text{CH}_3\text{CH}_2\text{Co}^{\text{III}}\text{Pc}$ has been synthesized and studied since alkyl

group effect, however confined to two alkyl groups, provides an important mechanistic tool. Any piece of evidence in favor or against the $\text{S}_{\text{N}}2$ mechanism is of value because of lingering uncertainty about the mechanism of methyl transfer from methylcobalt(III) complexes.²³

Experimental Section

Solutions of $\text{RCo}^{\text{III}}\text{Pc}$ complexes are photolabile and were handled at very reduced light level. The UV-visible spectra are insensitive to the presence of oxygen either at $\sim 1 \times 10^{-3}$ (measured in a thin cell) or $\sim 1 \times 10^{-5}$ M concentration level (measured in a 1-cm cell).

Materials. Methylcobalt(III) phthalocyanine was prepared as described earlier.¹⁰ Ethylcobalt(III) phthalocyanine was obtained by treating a DMA solution of $\text{Co}^{\text{I}}\text{Pc}^-$ with excess ethyl iodide at room temperature. After 10 min, the reaction mixture was poured into ice-cold water, and the precipitate was collected by filtration and washed with an abundance of water and ethanol. The crude material was chromatographed (SiO_2/DMA or $\text{SiO}_2/\text{toluene}$). Final purification involved saturation of a dimethylacetamide solution of the product with ethanol, which yielded material lacking axially coordinated solvent. ¹H NMR (pyridine-*d*₅, 300 MHz): δ -3.79 (t, 3H, $J = 7.6$ Hz), -3.47 (q, 2H, $J = 7.6$ Hz), 8.16–8.19 (m, 8H), 9.68–9.71 (m, 8H). Single-crystal X-ray structure of $\text{CH}_3\text{Co}^{\text{III}}\text{Pc}$ will be published elsewhere.²⁹

All solvents and reagents were supplied by Aldrich unless indicated differently. Dimethylacetamide (DMA), dimethylformamide (DMF), dimethyl sulfoxide (DMSO), and sulfolane (tetramethylene sulfone), all spectrometric grade solvents, were distilled under reduced pressure over CaH_2 and stored in an atmosphere of argon. A eutectic mixture of sulfolane and methyl sulfone was used for kinetic measurements to lower the melting point of the solvent.³⁰ Pyridine, piperidine, and *N*-methylpiperidine were purified by standard methods.

2-Methylpyridine was purified by the low-temperature Co(III) affinity distillation technique of Marzilli et al.³¹ Five consecutive distillation cycles were performed. This resulted in a formation constant for $\text{CH}_3\text{Co}^{\text{III}}\text{Pc}(2\text{-Mepy})$ lower by a factor of 3.5 from an erroneous value obtained with the ligand purified by regular distillation.

4-(Dimethylamino)pyridine was sublimed under reduced pressure. *N*-Methylimidazole (double distilled), methyl thiocyanate, and methyl isothiocyanate were used as received. Tributylphosphine (Fluka) was stored in a vial sealed with a Teflon-coated septum under argon. Triphenylphosphine was recrystallized from ethanol. Sodium iodide, tetrabutylammonium bromide, and tetrabutylammonium thiocyanate were good grade reagents, dried under vacuum. Potassium selenocyanate contained cyanide contaminant, which could not be removed completely by recrystallization from ethanol. Traces of strongly binding cyanide ligand interfered with selenocyanate-induced methyl transfer from cobalt.

Solutions of $\text{CH}_3\text{Co}^{\text{III}}\text{Pc}$ in donor solvents were stable at room temperature for extended period of time, but in the case of the ethylcobalt compound, the stability was substantially lower and fresh solutions were always used. Dilute blue toluene solutions of both complexes undergo a bleaching reaction at room temperature in a month or two, yielding an orange product. Addition of pyridine

(29) Galezowski, W.; Kubicki, M. paper in preparation.

(30) Lewis, E. S.; Kukes, S.; Slater, C. D. *J. Am. Chem. Soc.* **1980**, *102*, 303.

(31) Trommel, J. S.; Warncke, K.; Marzilli, L. G. *J. Am. Chem. Soc.* **2001**, *123*, 3358.

Table 1. Oxidation and Reduction Potentials (V vs Fc^+/Fc Couple) for $\text{RCo}^{\text{III}}\text{Pc}(\text{L})$ in DMF^a

R	L	first oxidn ^b	first redn ^c	second redn ^b
CH_3	DMF	0.34	-1.38	-1.91
CH_3	N-MeIm ^d	0.46	-1.38	-1.82
CH_3CH_2	DMF	0.33	-1.36	-1.92
CH_3CH_2	N-MeIm ^e	0.41	-1.38	-1.82

^a Potentials measured at platinum electrode with 0.2 M TBAP as supporting electrolyte. Scan rate, 0.1 V/s. ^b $(E_{\text{pc}} + E_{\text{pa}})/2$. ^c E_{pc} . ^d [N-MeIm] = 0.25 M. ^e [N-MeIm] = 0.75 M.

to the faintly orange solutions did not restore the blue color, which proves that the decay did not lead to precipitation of $\text{Co}^{\text{II}}\text{Pc}$, but a cleavage of the phthalocyanine system occurred. The presence of air had no effect on visible spectra of $\text{CH}_3\text{Co}^{\text{III}}\text{Pc}$ and $\text{CH}_3\text{CH}_2\text{-CoPc}$. Nevertheless, the solutions were deaerated with argon to prevent side processes, which was particularly important for experiments with phosphines, known to undergo oxidation by air. Such solutions still contained, however, sufficient amounts of oxidants to turn dilute $\text{Co}^{\text{I}}\text{Pc}^-$ into $\text{Co}^{\text{II}}\text{Pc}$ species.

Cyclic Voltammetry. CV was carried out under an atmosphere of argon by using a conventional three-electrode cell. Platinum wires were used as a working and counter electrode. A silver wire served as a quasi-reference electrode.³² Electrochemical data were obtained with an Autolab potentiostat. Tetrabutylammonium perchlorate (TBAP; 0.2 M) was used as a supporting electrolyte. Commercial TBAP was recrystallized from ethanol and dried in vacuo. The potentials were measured versus (Fc^+/Fc) couple (+ 0.40 V vs SCE in DMF).³³

Equilibrium and Kinetic Measurements. Except for temperature-jump and stopped-flow experiments, all spectrophotometric equilibrium and kinetic measurements were performed in a HP 8452 diode array spectrophotometer fitted with a Peltier temperature controller.

Equilibria were measured by titration of a $\text{RCo}^{\text{III}}\text{Pc}$ solution with neat ligand or ligand solution in a 1-cm spectrophotometric cell. The absorption changes were measured at λ_{max} of a difference spectrum in the 370–550 nm wavelength range (Table 2). Diagnostic plots of $\log[(A - A_0)/(A - A_f)]$ versus [ligand], where A_0 is the initial absorbance and A_f the value extrapolated for infinite ligand concentration, gave unity slope straight lines in accord with formation of a 1:1 complex. Should the substrate exist primarily as a dimer, the plots of $\log[(A - A_0)^2/(A_f - A)]$ versus [ligand] would give a straight line with a slope of 2, which is not the case (see the plots in Supporting Information). The absorbance values were corrected for dilution. Benesi–Hildebrand formalism³⁴ was used to determine equilibrium constants and molar absorptivities ($\Delta\epsilon$ in fact) with ligand in large excess over $\text{RCo}^{\text{III}}\text{Pc}$. In some cases the equilibria were measured over a range of temperatures (minimum four temperatures over a 30 °C temperature range) yielding reaction parameters shown in Table 2. At temperatures used for equilibrium measurements, the Co–C bond was stable.

Rates of Alkyl Transfer. The transfer rates from $\text{RCo}^{\text{III}}\text{Pc}$ to nucleophiles were measured spectrophotometrically under pseudo-first-order conditions, i.e., in excess nucleophile and added ligand, where applicable. Under these conditions, the methyl transfer

reaction is first order in organometallic substrate. Concentrations of $\text{RCo}^{\text{III}}\text{Pc}$ were usually $(6\text{--}8) \times 10^{-6}$ M. The major spectral change upon dealkylation of $\text{RCo}^{\text{III}}\text{Pc}$ complexes is a drop in the Q-band absorbance (see Figure S1, Supporting Information). Consequently, the absorption changes in the 660-nm region were used for rate determinations. In each case, a difference spectrum indicated the best wavelength.¹⁰ Six-wavelength kinetics mode of HP 8452 was used throughout this work, and the rates determined from the drop in Q-band were in general agreement with those determined from absorption increase in the high-energy region around 330 nm. With appropriate choice of scan time and the number of data points, monitoring light of HP 8452 did not cause photolysis on a scale that could interfere with measurements of the rates of alkyl transfer.

Usually the conditions were not strictly anaerobic. However, occasionally control runs were performed under rigorously anaerobic conditions and no substantial differences in dealkylation rate constants were found. In those dilute ($\sim 1 \times 10^{-5}$ M) thoroughly deaerated solutions, only a small fraction of the product existed as $\text{Co}^{\text{I}}\text{Pc}^-$ complex. When sampling was used (thiocyanate reaction), the samples were allowed to oxidize completely with atmospheric oxygen on cooling in a spectrophotometric cell. Alternatively, the sample was quenched with a small volume of sodium cyanide solution to turn $\text{RCo}^{\text{III}}\text{Pc}$, $\text{Co}^{\text{II}}\text{Pc}$, and $\text{Co}^{\text{I}}\text{Pc}^-$ into a mixture of $\text{RCo}^{\text{III}}\text{Pc}(\text{CN})^-$ and $\text{Co}^{\text{III}}\text{Pc}(\text{CN})_2^-$. The spectra of the two latter display many differences.³⁵ Dealkylation of $\text{RCo}^{\text{III}}\text{Pc}(\text{CN})^-$ is negligibly slow.¹⁰ The two procedures led to the same results. Rates observed in dilute solutions agreed semiquantitatively with changes undergoing in concentrated solutions in NMR probe or during product isolations. The initial demethylation product, $\text{Co}^{\text{I}}\text{Pc}^-$, was not observed in kinetic runs, where $[\text{RCo}^{\text{III}}\text{Pc}] \sim 1 \times 10^{-5}$ M. Its presence was, however, evident when concentration of the cobalt complex was $\sim 1 \times 10^{-3}$ M in thoroughly deoxygenated solutions, e.g., in product identification assays. A similar situation was previously described for the iodide and bromide reaction.¹⁰ Also Hogenkamp and co-workers did not observe postulated Co(I) product of dealkylation under anaerobic conditions.³⁴ Other workers observed Co(I) product only in the presence of borohydride.⁵

With nucleophiles that do not coordinate to the cobalt center (iodide, bromide in coordinating solvents, triphenylphosphine) the second-order rate constants, k_2 , were determined from the slopes of k_{obs} versus [Nu] usually for at least five concentrations of the nucleophile. In some cases of extremely slow reactions in DMSO and DMF, after linear dependence of k_{obs} versus [Nu] had been determined at one temperature, k_2 values for other temperatures were calculated as $k_{\text{obs}}/[\text{Nu}]$ for a large [Nu]. When a nucleophile formed inactive $\text{RCo}^{\text{III}}\text{Pc}(\text{Nu})$ complex, a double-reciprocal plot of $1/k_{\text{obs}}$ versus $1/[\text{Nu}]$ gave a slope equal $1/k_2$ and an intercept K_{Nu}/k_2 (eq 6), from which the second-order rate constant for nucleophile-free substrate and stability constant of $\text{RCo}^{\text{III}}\text{Pc}(\text{Nu})$ were found.

$$\frac{1}{k_{\text{obs}}} = \frac{1}{k_2[\text{Nu}]} + \frac{K_{\text{Nu}}}{k_2} \quad (6)$$

In this case, a larger number of points and a broad range of nucleophile concentration is needed to achieve reasonable accuracy of k_2 and K_{Nu} .

(32) Nevin, W. A.; Hempstead, M. R.; Liu, W.; Leznoff, C. C.; Lever, A. B. P. *Inorg. Chem.* **1987**, *26*, 570.

(33) Lever, A. B. P.; Milaeva, E. R.; Speier, G. In *Phthalocyanines. Properties and Applications*; Leznoff, C. C., Lever A. B. P., Eds.; Wiley-VCH: New York, 1993; Vol 3, Chapter 1, p 8.

(34) Benesi, H. A.; Hildebrand, J. H. *J. Am. Chem. Soc.* **1949**, *71*, 2703.

(35) Day, P.; Hill, H. A. O.; Price, M. G. *J. Chem. Soc. A* **1968**, 90.

Table 2. Thermodynamic Data for Ligand Binding to RCo^{III}Pc

axial R	ligands L	solvent	λ_{\max}^a (nm)	K_L^b (M ⁻¹)	ΔH (kcal/mol)	ΔS (cal mol ⁻¹ K ⁻¹)
Me	py	DMA	416	42 ± 1	-4.0 ± 0.3	-6 ± 1
Et	py	DMA	416	30 ± 1	nd ^d	nd
Me	py	DMF	418	31 ± 1	-3.6 ± 0.2	-5.1 ± 0.7
Me	py	DMSO	424	5.9 ± 0.1	-4.5 ± 0.1	-11.7 ± 0.4
Me	py	sulfolane	414	1 110 ± 60	-7.5 ± 0.2	-11.2 ± 0.3
Me	py	CH ₂ Cl ₂	400	3 630 ± 60	nd	nd
Me	py	toluene	402	2 410 ± 50	-9.8 ± 0.2	-17.0 ± 0.7
Et	py	toluene	414	340 ± 10	-7.7 ± 0.5	-14 ± 2
Me	2-Mepy	toluene	392	2.6 ± 0.1	nd	nd
Me	4-Mepy	toluene	402	4 600 ± 100	nd	nd
Me	4-CNpy	toluene	390	400 ± 20	nd	nd
Me	4-NMe ₂ py	DMA	424	1 840 ± 70	nd	nd
Me	4-NMe ₂ py	toluene	418	94 000 ± 2000	nd	nd
Me	N-MeIm	DMA	424	2 000 ± 20	-7.4 ± 0.2	-9.9 ± 0.5
Et	N-MeIm	DMA	430	790 ± 20	-6.4 ± 0.6	-8 ± 2
Me	N-MeIm	DMSO	426	146 ± 5	-6.1 ± 0.5	-10 ± 2
Me	N-MeIm	sulfolane	420	19 100 ± 400	nd	nd
Me	N-MeIm	toluene	414	55 000 ± 900	-11.5 ± 0.3	-16.9 ± 0.9
Et	N-MeIm	toluene	424	8 450 ± 20	-10.5 ± 0.2	-17.2 ± 0.7
Me	piperidine	DMA	434	710 ± 10	-6.2 ± 0.3	-7.7 ± 0.8
Et	piperidine	DMA	446	425 ± 6	nd	nd
Me	piperidine	toluene	424	6 940 ± 20	-11.8 ± 0.3	-22 ± 1
Et	piperidine	toluene	436	1 370 ± 20	-10.8 ± 0.3	-21.7 ± 0.9
Me	N-Mepiperidine	toluene	422	14.2 ± 0.2	-9.4 ± 0.4	-26 ± 1
Me	DABCO	toluene	442	12 900 ± 300	nd	nd
Me	DABCO	DMA	450	142 ± 1	-7.9 ± 0.2	-8.0 ± 0.8
Me	PBu ₃	toluene	510	350 ± 30	nd	nd
Et	PBu ₃	toluene	522	123 ± 6	nd	nd
Me	H ₂ O	DMA	380	1.9 ± 0.1	nd	nd
Et	H ₂ O	DMA	394	1.88 ± 0.02	nd	nd
Me	DMA	toluene	384	5.1 ± 0.2	-3.8 ± 0.1	-9.7 ± 0.2
Me	DMF	toluene	384	6.8 ± 0.1	nd	nd
Me	DMSO	sulfolane	388	6.3 ± 0.8	nd	nd
Me	DMSO	toluene	380	47.2 ± 0.3	-6.0 ± 0.2	-12.4 ± 0.8
Me	THF	toluene	374	5.9 ± 0.2	nd	nd
Me	Me ₂ S	sulfolane	434	6.3 ± 0.2	-5.5 ± 0.6	-15 ± 2
Me	Me ₂ S	toluene	430	9.6 ± 0.1	-8.0 ± 0.9	-22 ± 3
Me	SCN ⁻	DMA	424	23.9 ± 0.6	nd	nd
Me	SCN ⁻	sulfolane	412	173 ± 4	nd	nd
Me	SCN ⁻	toluene ^c	412	39 ± 2	nd	nd

^a λ_{\max} of difference spectra in the 370–540 nm range at which equilibria were measured. ^b A result of Benesi–Hildebrand treatment (25 °C); the difference in molar absorptivities: 5000 < $\Delta\epsilon$ < 12 000 (lower values are measured in coordinating solvents). ^c Tetrabutylammonium salt. ^d nd, not determined.

As follows from eq 5, in the presence of an axial base, L, unable to attack the Co–C bond, and at constant concentration of nucleophile Nu, a plot of $1/k_{\text{obs}}$ versus [L] should give a slope K_L/k_2 (eq 7), which worked well for thiocyanate reaction in DMA in the presence of variable concentrations of pyridine.

$$\frac{1}{k_{\text{obs}}} = \frac{1}{k_2[\text{Nu}]} + \frac{K_{\text{Nu}}}{k_2} + \frac{K_L[\text{L}]}{k_2[\text{Nu}]} \quad (7)$$

Equation 7 is further simplified when the nucleophile does not coordinate to the organometallic substrate. In this case, a linear plot of $[\text{Nu}]/k_{\text{obs}}$ versus [L] ($k_{\text{obs}}/[\text{Nu}]$) at a constant [L] may be regarded here as an apparent second-order rate constant k_2^{app} yields a slope of K_L/k_2 (eq 8).

$$\frac{1}{k_2^{\text{app}}} = \frac{[\text{Nu}]}{k_{\text{obs}}} = \frac{1}{k_2} + \frac{K_L[\text{L}]}{k_2} \quad (8)$$

Since k_2 can be accurately determined in the absence of L, K_L values calculated from the slope are available for comparison to those obtained from equilibrium studies. Should the value determined from kinetics be smaller than the equilibrium K_L , a contribution from RCo^{III}Pc(L) species to the rate of dealkylation would be

indicated. Related eq 9 is also useful for studying axial base inhibition

$$k_2^{\text{app}} = \frac{k_2}{K_L[\text{L}] + 1} \quad (9)$$

Conductances of Bu₄NCSN. Bu₄NCSN conductances in DMA (25.0 °C) and sulfolane (30.0 °C) were measured in a conventional platinum electrode conductometric cell protected from moisture and air and immersed in an oil-filled thermostat using a Tesla BM 484 bridge operated at 1592 Hz. The cell temperature was maintained constant within 0.1 °C. The concentration range 0.00015–0.007 M and 0.00028–0.01 M in DMA and sulfolane, respectively, covered concentration ranges used in the kinetic studies. The Kohlrausch plots (available in Supporting Information), Λ versus $c^{1/2}$, were straight lines with slopes, α , close to their theoretical values: in DMA, $\alpha = 128 \pm 6$ (theoretical value is 132.4) and $\Lambda_0 = 70.9 \pm 0.4$; in sulfolane, $\alpha = 13.5 \pm 0.3$ (theoretical $\alpha = 14.13$) and $\Lambda_0 = 12.66 \pm 0.03$. All values are given in conventional units.

Temperature Jump Measurements. The measurements were performed using a Hi-Tech Scientific IS-2 instrument by monitoring absorbance changes at 420-nm CH₃Co^{III}Pc(py) absorption band. CH₃Co^{III}Pc solutions in DMA contained varied amounts of pyridine

(0.0124–0.053 M). At concentrations of pyridine used, comparable amounts of $\text{CH}_3\text{Co}^{\text{III}}\text{Pc}(\text{py})$ and $\text{CH}_3\text{Co}^{\text{III}}\text{Pc}(\text{DMA})$ existed in solution. The solutions were 0.2 M in TBAP. The presence of TBAP had little effect on the stability constant for $\text{CH}_3\text{Co}^{\text{III}}\text{Pc}(\text{py})$. Concentration of the complex was large ($\sim 5 \times 10^{-4}$ M) to achieve a satisfactory signal-to-noise ratio. Temperature rise (~ 15 °C) was calculated using known capacitance, voltage across capacitors, specific heat of DMA, and mass of the sample. The solution in the spectrophotometric cell was illuminated only during data acquisition.

Product Identification Assays. A HP 5890 II gas chromatograph, equipped with a FID was used for determinations of volatile products. Samples of the gas phase over solution were chromatographed on a 2.5 m \times 1/8 in. packed column (HAYE SEP Q) 90 °C(2min), 90–150 °C (10 °C/min). For determination of $\text{CH}_3\text{-SCN}$, a 30 m \times 0.53 mm \times 0.88 μm HP-1 was used (oven temperature 90 °C).

$\text{CH}_3\text{Co}^{\text{III}}\text{Pc}$ with SCN^- in DMA. $\text{CH}_3\text{Co}^{\text{III}}\text{Pc}$ (12 mg; 0.02 mmol) and Bu_4NSCN (92 mg; 0.31 mmol) were dissolved in 25 mL of DMA under argon and kept in a tightly stoppered flask for 120 h at room temperature. The solution gradually turned yellow-green. A small portion was siphoned under argon into a thin cell (0.1 mm). A spectrum of $\text{Co}^{\text{I}}\text{Pc}^-$ was obtained, the intensity of which at 700 nm corresponded to a 95% yield. To 20 mL of the remaining solution, 1 μL of toluene internal standard was added. A half-volume of the solution was bulb-to-bulb distilled, and the distillate was gas chromatographed. The yield of CH_3SCN was 91% while no trace of CH_3NCS was detected. Taking into account the approximate half-life time of ~ 30 h estimated from $k_2^{25^\circ\text{C}}$ and the stability constant for $\text{CH}_3\text{Co}^{\text{III}}\text{Pc}(\text{SCN})^-$, the yield is consistent with the results of kinetic measurements.

$\text{CH}_3\text{CH}_2\text{Co}^{\text{III}}\text{Pc}$ with SCN^- in DMA. A solution of $\text{CH}_3\text{CH}_2\text{-Co}^{\text{III}}\text{Pc}$ (12 mg; 0.02 mmol) and Bu_4NSCN (39 mg; 0.13 mmol) in 10 mL of DMA was sealed in a vial under Ar. The solution did not change color overnight. In the course of the subsequent 10-h incubation at 60 °C, it gradually turned yellow-green. Gas phase over the solution was subjected to GC analysis for light hydrocarbons. Ethylene (5%) and ethane (1%) were found. A small part of the yellow-green solution was transferred under Ar into a 0.1-mm cell, and a visible spectrum of $\text{Co}^{\text{I}}\text{Pc}^-$ was obtained (95% yield). The yield of $\text{CH}_3\text{CH}_2\text{SCN}$ determined as described above was 86%.

$\text{CH}_3\text{Co}^{\text{III}}\text{Pc}$ with PPh_3 in DMSO- d_6 . A solution of $\text{CH}_3\text{Co}^{\text{III}}\text{Pc}$ (0.8 mg; 0.0014 mmol) and PPh_3 (50 mg, 0.19 mmol) in 0.7 mL of DMSO- d_6 was sealed in an NMR tube under Ar. Initially ^1H NMR resonances of $\text{CH}_3\text{Co}^{\text{III}}\text{Pc}$ appeared to be unaffected by the presence of the phosphine. ^1H NMR (DMSO- d_6 , 300 MHz): δ -4.79 (br s, 3H), 8.24–8.27 (m, 8H), 9.43–9.46(m, 8H). The broad axial methyl resonance vanished overnight while a doublet at $\delta = 3.145$ ($J = 14.7$ Hz) appeared, indicating formation of triphenylmethylphosphonium ion.³⁶ The contents of the NMR tube turned yellow-green, and phthalic signals of $\text{CH}_3\text{Co}^{\text{III}}\text{Pc}$ were replaced by resonances characteristic of $\text{Co}^{\text{I}}\text{Pc}^-$. The half-life of $\text{CH}_3\text{Co}^{\text{III}}\text{Pc}$ in this experiment was ~ 5 h.

$\text{CH}_3\text{CH}_2\text{Co}^{\text{III}}\text{Pc}$ with PPh_3 in DMA. A solution of $\text{CH}_3\text{CH}_2\text{-Co}^{\text{III}}\text{Pc}$ (12 mg; 0.02 mmol) and PPh_3 (290 mg; 1.1 mmol) in 10 mL of DMA was sealed in a vial under argon and kept at room temperature in the dark for 70 h. A UV–visible spectrum of the resulting solution in a thin cell indicated a 100% $\text{Co}^{\text{I}}\text{Pc}^-$ yield. GC analysis of the gas phase gave ethylene (4.5%) and ethane (0.3%). The liquid phase was combined with excess water, then

filtered, acidified with HCl, and evaporated to dryness in vacuo. The residue was extracted with CDCl_3 (1 mL) in which it only partially dissolved. In the ^1H NMR spectrum of the remainder in D_2O , two sets of signals of ethyl group bound to phosphorus were found, one of which corresponded to the literature $^1\text{HNMR}$ spectrum of $\text{CH}_3\text{CH}_2\text{PPh}_3\text{I}$.³⁶

$\text{CH}_3\text{CH}_2\text{Co}^{\text{III}}\text{Pc}$ with PBu_3 in DMA. A solution of $\text{CH}_3\text{CH}_2\text{-Co}^{\text{III}}\text{Pc}$ (12 mg; 0.02 mmol) and PBu_3 (30 μL ; 0.12 mmol) in 10 mL of DMA was sealed in a vial under Ar and kept at room temperature in the dark for 70 h. A $\text{Co}^{\text{I}}\text{Pc}^-$ spectrum measured in a thin cell corresponded to a 95% yield. GC analysis of gaseous products ethylene (1.9%) and ethane (0.5%) was performed. The liquid was worked up as described above. ^1H NMR spectrum of D_2O solution was consistent with that for ethyltributylphosphonium.³⁶

$\text{CH}_3\text{Co}^{\text{III}}\text{Pc}$ with Piperidine in DMSO- d_6 . A solution of $\text{CH}_3\text{-Co}^{\text{III}}\text{Pc}$ (0.8 mg; 0.0014 mmol) and piperidine (2 μL ; 0.02 mmol) in 0.7 mL of DMSO- d_6 exhibited a spectrum indicating partial coordination of piperidine to cobalt. $^1\text{HNMR}$ (DMSO- d_6 , 300 MHz): δ -5.02 (br s, 3H), 8.21–8.25 (m, 8H), 9.41–9.44 (m, 8H). Upon overnight heating at 70 °C, precipitation of a blue solid occurred. The supernatant solution was transferred into another NMR tube. Apart from residual signals of $\text{CH}_3\text{Co}^{\text{III}}\text{Pc}(\text{pip})$ and the spectrum of unreacted piperidine, resonances identical to those of authentic *N*-methylpiperidine in DMSO- d_6 at δ 2.10 (s, 3H) and 2.22 (br s, 4H) were observed. Apparently *N*-methylpiperidinium had been deprotonated by excess piperidine.

$\text{CH}_3\text{CH}_2\text{Co}^{\text{III}}\text{Pc}$ with Piperidine in DMSO- d_6 . In an experiment analogous to that described above, $\text{CH}_3\text{CH}_2\text{Co}^{\text{III}}\text{Pc}$ with piperidine was heated in an NMR tube. Initial spectrum, $^1\text{HNMR}$ (DMSO- d_6 , 300 MHz): δ -4.19 (t, 3H, $J = 7.2$ Hz), -3.99 (br- q, 2H), 8.22–8.25 (m, 8H), 9.41–9.44 (m, 8H). After overnight incubation at 70 °C, the axial ethyl signals disappeared from the spectrum.

$\text{CH}_3\text{Co}^{\text{III}}\text{Pc}$ with Triethylamine in DMSO- d_6 . A solution of $\text{CH}_3\text{Co}^{\text{III}}\text{Pc}$ (0.8 mg; 0.0014 mmol), triethylamine (2 μL ; 0.014 mmol), and benzene internal standard (2 μL) in 0.7 mL of DMSO- d_6 exhibited an unchanged $^1\text{HNMR}$ spectrum of $\text{CH}_3\text{Co}^{\text{III}}\text{Pc}$ indicating no coordination of TEA to cobalt. After overnight heating at 70 °C, axial methyl and phthalic protons resonances disappeared from the spectrum while signals identical with those of methyl-triethylammonium iodide in DMSO- d_6 corresponding to $100 \pm 10\%$ yield built up.

NMR. NMR spectra were recorded on a Varian Gemini 300 VT instrument. Due to poor solubility of $\text{RCo}^{\text{III}}\text{Pc}$ in noncoordinating solvents, DMSO- d_6 and DMF- d_7 were the solvents of choice.

Results and Discussion

Cyclic voltammetry of $\text{CH}_3\text{Co}^{\text{III}}\text{Pc}$ in noncoordinating solvents is not viable because of inadequate solubility. In DMF, the molecule undergoes two reductions and one oxidation within the limit of the solvent (Figure 1). The oxidation and the second reduction are quasi-reversible while the first reduction is irreversible (up to the scan rate of 30 V/s). The second reduction potential is consistent with the value reported for ring reduction of $\text{Co}(\text{I})\text{Pc}(-2)/\text{Co}(\text{I})\text{Pc}(-1)$ couple.³⁷ A new oxidation peak is observed at -0.75 V only after $\text{CH}_3\text{Co}^{\text{III}}\text{Pc}$ has been reduced at -1.38 V. Potential of this oxidation is consistent with literature data for $\text{Co}^{\text{I}}\text{Pc}^-$ in DMF.³⁷ Hence, the irreversibility of the first

(36) Hendrickson, J. B.; Maddox, M. L.; Sims, J. J.; Kaesz, H. H. *Tetrahedron* **1964**, *20*, 449.

(37) Clack, D. W.; Hush, N. S.; Woolsey, I. S. *Inorg. Chim. Acta* **1976**, *19*, 129.

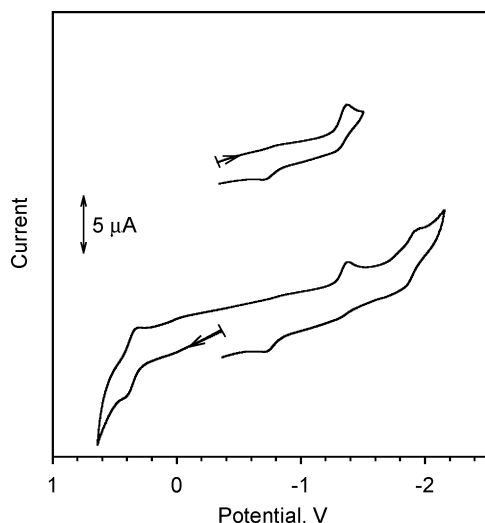


Figure 1. Cyclic voltammograms for $\text{CH}_3\text{Co}^{\text{III}}\text{Pc}$ in DMF. Scan rate, 0.1 V/s. Potentials versus Fc^+/Fc couple. $[\text{CH}_3\text{Co}^{\text{III}}\text{Pc}] = 2 \times 10^{-4}$ M. $[\text{TBAP}] = 0.2$ M.

reduction seems to be caused by fast decomposition of one-electron reduced $\text{CH}_3\text{Co}^{\text{III}}\text{Pc}$ with formation of $\text{Co}^{\text{I}}\text{Pc}^-$ (an EC process). Cyclic voltammograms for $\text{CH}_3\text{CH}_2\text{Co}^{\text{III}}\text{Pc}$ are very similar to those for $\text{CH}_3\text{Co}^{\text{III}}\text{Pc}$. In the presence of added N-MeIm axial base the oxidation and second reduction peaks are shifted anodically by ~ 0.1 V (Table 1). This shift comes unexpected especially when the oxidation is considered, since logically it would be consistent with better electron donation properties of DMF than N-MeIm. The difference between the first oxidation and the second reduction potential of ~ 2.25 V is similar to that of ring oxidation and reduction of various substituted $\text{Co}(\text{II})$ phthalocyanines in donor solvents³⁸ or that of $\text{CH}_3\text{Co}^{\text{III}}(\text{TPP})$.³⁹ However, further research is needed to claim with reasonable confidence that this gap corresponds to the difference between HOMO and LUMO of the phthalocyanine macrocycle.

First reduction potentials for $\text{RCo}^{\text{III}}\text{Pc}$ (Table 1), as well as those for the related TPP complexes,³⁹ little change on replacement of methyl by ethyl axial ligand. These potentials also virtually do not change on addition of strongly binding N-MeIm, which is consistent with prevalently six-coordinate species in DMF, since the five-coordinate form should be easier reduced. The potential shift between five- and six-coordinate RCoPc is of interest, but the question whether it will be as small as ~ 0.1 V observed on transfer of $\text{RCo}(\text{TPP})$ complexes from CH_2Cl_2 to pyridine or, more likely, it will be larger must await a study on a phthalocyanine complex sufficiently soluble in nonbinding solvents.

Disregarding differences in solvents, scan rates used, etc., it may be concluded that the first reduction potential, ~ -1 V versus SCE (Fc^+/Fc couple is 0.40 V versus SCE),³³ is similar to those for σ -bonded alkyl-Costa-type models, which are at the anodic extreme of the literature reduction potentials for alkylcobalt(III) models.⁴⁰ $\text{CH}_3\text{Co}^{\text{III}}\text{Pc}$ is reduced at

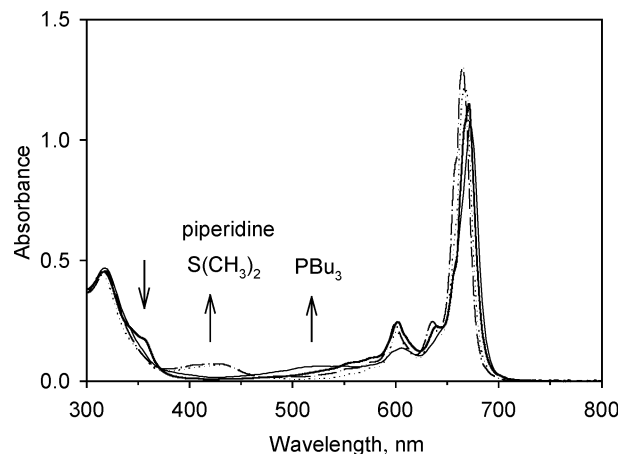


Figure 2. Representative spectral changes on $\text{CH}_3\text{Co}^{\text{III}}\text{Pc}$ ligation in toluene: $\text{CH}_3\text{Co}^{\text{III}}\text{Pc}$ (thick solid line); $\text{CH}_3\text{Co}^{\text{III}}\text{Pc}(\text{L})$, L = piperidine (dashed), L = $(\text{CH}_3)_2\text{S}$ (dotted); L = PBu_3 (solid). $[\text{CH}_3\text{Co}^{\text{III}}\text{Pc}(\text{L})] = 7 \times 10^{-6}$ M.

potentials by 0.4, 0.51, and 0.46 V less negative than five-coordinate $\text{CH}_3\text{Co}(\text{TPP})$ in CH_2Cl_2 ,³⁹ $\text{CH}_3\text{CH}_2\text{Co}(\text{TPP})(\text{py})$ in pyridine,³⁹ and 90% six-coordinate MeCbi^+ in aqueous solution,⁴¹ respectively. The ~ 0.5 -V shift in reduction potentials between six-coordinate alkylcobalt(III) TPP and phthalocyanine complexes reflects mainly different properties of the equatorial systems, the trans axial ligation is of secondary importance.

UV–Visible Spectra. The UV–visible spectra of cobalt phthalocyanines are dominated by Q and B bands.⁴² The Q-band is more intense in the spectra of $\text{RCo}^{\text{III}}\text{Pc}$ ($\epsilon \sim 180\,000$ cm^{-1} M^{-1}) than $\text{Co}^{\text{II}}\text{Pc}$ complexes.¹⁰ A blue shift of the Q-band in the spectrum of $\text{CH}_3\text{Co}^{\text{III}}\text{Pc}$ is observed upon transfer from toluene (λ_{max} 671 nm) to polar solvents: sulfolane (666 nm), DMSO (666 nm), DMF and DMA (660 nm). Similar blue shifts occur in the course of trans axial ligation of $\text{RCo}^{\text{III}}\text{Pc}$ complexes with various ligands in toluene (Figure 2). Relatively weak absorption, λ_{max} in the 380–410 nm range, $\epsilon \sim 10\,000$ cm^{-1} M^{-1} observed in coordinating polar aprotic solvents (Figure 3) with only a cursory glance may go unnoticed. However, in this wavelength range hexacoordinate $\text{RCo}^{\text{III}}\text{Pc}(\text{L})$ complexes do absorb. Upon dealkylation, leading essentially to five-coordinate $\text{Co}^{\text{II}}\text{Pc}(\text{L})$ or $\text{Co}^{\text{II}}\text{Pc}(\text{solvent})$ products, absorption bands in this wavelength range disappear (see Figure S1 in Supporting Information). Absorption bands in the spectra of $\text{CH}_3\text{CH}_2\text{Co}^{\text{III}}\text{Pc}$ are as a rule slightly red-shifted from those for $\text{CH}_3\text{Co}^{\text{III}}\text{Pc}$. The spectra of presumably five-coordinate $\text{RCo}^{\text{III}}\text{Pc}$ species in toluene and CH_2Cl_2 display a 354-nm shoulder on the longer wavelength side of the B band (Figures 2, 3, and S2) of intensity comparable to the weak absorption bands in coordinating solvents. Upon trans axial ligation of $\text{RCo}^{\text{III}}\text{Pc}$ the 354-nm shoulder disappears with concomitant formation of a longer wavelength band, λ_{max} of which depends significantly on the identity of the ligating atom (Figures 2 and S2, Table 2). The weak absorption

(38) Reference 33, p 47.

(39) Kadish, K. M.; Han, B. C.; Endo, A. *Inorg. Chem.* **1991**, *30*, 4502.

(40) Costa, G.; Puxeddu, A.; Reisenhofer, E. *J. Chem. Soc., Dalton Trans.* **1972**, 1519.

(41) Lexa, D.; Savéant, J.-M. *J. Am. Chem. Soc.* **1978**, *100*, 3220.

(42) Kobayashi, N.; Konami, H. In *Phthalocyanines. Properties and Applications*; Leznoff, C. C., Lever, A. B. P., Eds.; Wiley-VCH: New York 1996; Vol. 4, Chapter 9.

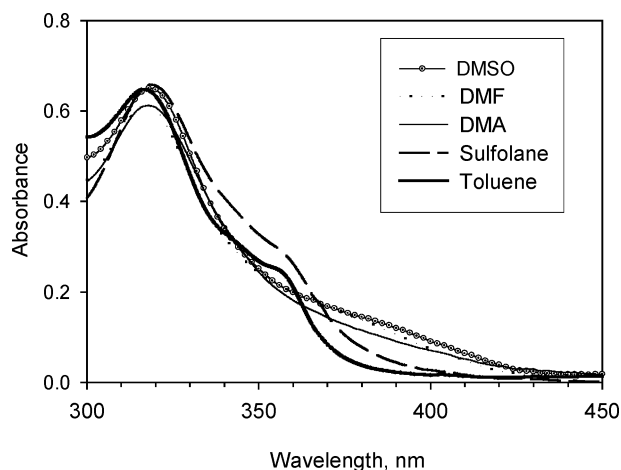


Figure 3. Solvent effect on UV-visible spectra of $\text{CH}_3\text{Co}^{\text{III}}\text{Pc}$. $[\text{CH}_3\text{Co}^{\text{III}}\text{Pc}] = 1 \times 10^{-5}$ M, 25°C .

bands, the position of which depends strongly on the nature of ligand, are reminiscent of similar UV-visible absorption of $\text{Co}^{\text{III}}\text{PcX}_2^-$ complexes ($X = \text{OH}, \text{F}, \text{Cl}, \text{Br}$) ascribed to X to Co CT transitions.^{43,44} The shifts of the Q-band are relatively small, and those of the B-band are negligible (Figures 2, 3, and S2). However, in the spectrum of the PBu_3 complex, the overtone at ~ 600 nm has about half the intensity exhibited with other ligands (Figure 2).

Solutions of some alkylcobinamides exhibit strong temperature spectral changes tentatively ascribed to reversible removal of coordinated water.²⁵ The possibility that a similar equilibrium would be observed in the case of weakly bound oxygenous ligand adducts with $\text{RCo}^{\text{III}}\text{Pc}$ seemed real. The spectra of $\text{RCo}^{\text{III}}\text{Pc}$ in DMA, DMF, DMSO, sulfolane, and toluene were recorded over a range of temperatures (mostly $5\text{--}80^\circ\text{C}$) to follow possible changes due to desolvation of $\text{RCo}^{\text{III}}\text{Pc}(\text{solvent})$. The spectra in toluene and sulfolane showed no temperature variations of interest. The weak absorption around 390 nm in DMSO and DMF decreased only slightly on heating. By contrast, in DMA a substantial reversible decrease in absorption on heating was observed (Figure 4; the details are given in Supporting Information). It is tempting to accept that in DMA at 25°C about half of $\text{CH}_3\text{Co}^{\text{III}}\text{Pc}$ persists as five-coordinate species, and at 80°C , the desolvation is very extensive.⁴⁵ However, conflicting evidence comes from very similar stability constants for $\text{CH}_3\text{Co}^{\text{III}}\text{Pc}(\text{DMA})$ and $\text{CH}_3\text{Co}^{\text{III}}\text{Pc}(\text{DMF})$ in toluene, and those for $\text{CH}_3\text{Co}^{\text{III}}\text{Pc}(\text{py})$ in DMA and DMF (Table 2). Also, the amount of five-coordinate species estimated from the formation constant for $\text{CH}_3\text{Co}^{\text{III}}\text{Pc}(\text{DMA})$ in toluene (vide infra) would be more than 1 order of magnitude smaller than suggested by the temperature-induced spectral changes. This and also electrochemical studies suggest extensive DMA coordination to $\text{CH}_3\text{Co}^{\text{III}}\text{Pc}$. The temperature-induced spectral

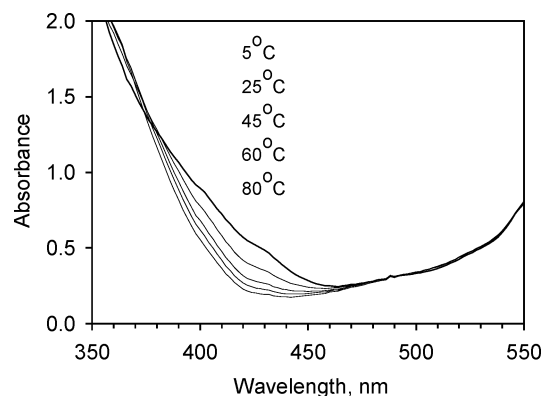


Figure 4. Thermochromism of $\text{CH}_3\text{Co}^{\text{III}}\text{Pc}$ in DMA solution. $[\text{CH}_3\text{Co}^{\text{III}}\text{Pc}] = 7 \times 10^{-5}$ M.

changes in DMA do not find an easy explanation within the concepts developed in this paper.

Coordination State of $\text{RCo}^{\text{III}}\text{Pc}$ in Solution. Since numerous alkylcobalt complexes exist as dimers in solution and in the solid,^{46,47} special attention has to be paid to the question of possible dimerization of $\text{RCo}^{\text{III}}\text{Pc}$. Dimeric structures of $\text{CH}_3\text{CH}_2\text{Co}^{\text{III}}\text{Pc}$ have been found in the solid,²⁹ but this does not automatically imply such substrate association in solution. Judging by interatomic distances in the $(\text{CH}_3\text{CH}_2\text{Co}^{\text{III}}\text{Pc})_2$ unit the interaction between the two molecules is a π -stacking; thus, $\text{RCo}^{\text{III}}\text{Pc}$ molecules preserve their five-coordinate structure in the dimer, which is not always the case with alkylcobalt complexes. Equilibrium studies of ligand binding by $\text{RCo}^{\text{III}}\text{Pc}$ are helpful for establishing monomeric structure of the complexes in solution. Diagnostic plots of $\log[(A - A_0)/(A_T - A)]$ versus $\log[\text{ligand}]$, invariantly give unity slopes (see Experimental Section and Figures S3–S7) in accordance with monomeric substrate. Fulfillment of the Beer law over broad ranges of the complex concentration, which is observed in donor solvents,¹⁰ could not be used as a criterion in toluene and sulfolane because of the poor solubility of $\text{RCo}^{\text{III}}\text{Pc}$ in these solvents.

The conviction of the pentacoordinate nature of $\text{RCo}^{\text{III}}\text{Pc}$ species in toluene gains support from the fact that analogous σ -bonded alkylcobalt(III) porphyrinic complexes have been shown to persist as five-coordinate species in aromatic hydrocarbons.⁴⁸ Difference spectra between $\text{RCo}^{\text{III}}\text{Pc}(\text{O-donor})$ complexes and $\text{RCo}^{\text{III}}\text{Pc}$ in toluene exhibit maximums at ~ 380 nm, which makes the possibility that $\text{RCo}^{\text{III}}\text{Pc}(\text{H}_2\text{O})$ species resulting from an interaction with adventitious water are mistaken for pentacoordinate $\text{RCo}^{\text{III}}\text{Pc}$ (the 354 -nm shoulder on the B band) less likely. The UV-visible spectra are similar in toluene, CH_2Cl_2 , and sulfolane, in which solvent solubility of $\text{RCo}^{\text{III}}\text{Pc}$ is ~ 100 -fold lower than in coordinating solvents, DMA, DMF, or DMSO. Hence, not only in toluene and CH_2Cl_2 , but also in polar sulfolane, the five-coordinate $\text{CH}_3\text{Co}^{\text{III}}\text{Pc}$ form is likely to prevail. Poor

(43) Homborg, H.; Kaltz, W. *Z. Naturforsch.* **1984**, *39 b*, 1490.

(44) Notably, low-energy absorptions of alkylcobaloximes between 400 and 500 nm, ascribed to $\text{Co}\text{--}\text{C}$ CT transition, show inverse dependence of λ_{max} on ligand donicity. Schrauzer, G. N.; Lee, L. P.; Siebert, J. W. *J. Am. Chem. Soc.* **1970**, *92*, 2997.

(45) Note also that, at 25°C , the weak absorption band has lower intensity than those in DMSO and DMF (Figure 2).

(46) Marzilli, L. G.; Summers, M. F.; Bresciani-Pahor, N.; Zangrando, E.; Charland, J.-P.; Randaccio, L. *J. Am. Chem. Soc.* **1985**, *107*, 6880.

(47) (a) Costa, G. *Pure Appl. Chem.* **1972**, *30*, 335. (b) Calligaris, M.; Minichelli, D.; Nardin, G.; Randaccio, L. *J. Chem. Soc. A* **1971**, 2720. (c) Courtright, R. L.; Drago, R. S.; Nusz, J. A.; Nozari, M. S. *Inorg. Chem.* **1973**, *12*, 2809 and references therein.

(48) Stolzenberg, A. M.; Summers, J. S. *Inorg. Chem.* **2000**, *39*, 1518.

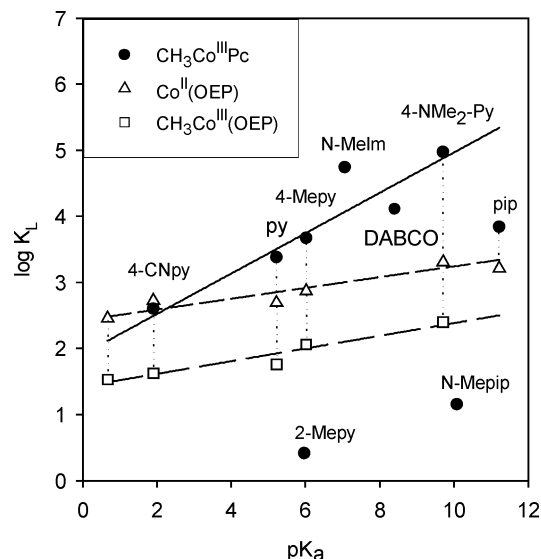


Figure 5. Equilibrium constants for coordination of nitrogenous bases to $\text{CH}_3\text{Co}^{\text{III}}\text{Pc}$ and related complexes in toluene. Data for $\text{CH}_3\text{Co}^{\text{III}}(\text{OEP})$ and $\text{Co}^{\text{II}}(\text{OEP})$ from refs 48 and 52, respectively. pK_a of protonated ligands in water from refs 52 and 49.

ligational properties of sulfones have also been observed earlier,¹⁴ when, unlike in DMA, ligation of Br ion by $\text{CH}_3\text{-Co}^{\text{III}}\text{Pc}$ was observed in sulfolane. Addition of sulfolane to a toluene solution of $\text{CH}_3\text{Co}^{\text{III}}\text{Pc}$ does not cause significant spectral changes, except the Q-band broadening, which is compatible with lack of trans axial complexation or an extremely weak interaction. Another argument for the existence of five-coordinate species in toluene and sulfolane lies in the fact that stability constants for $\text{RCo}^{\text{III}}\text{Pc}(\text{L})$ are much larger in noncoordinating solvents such as toluene, CH_2Cl_2 , and polar sulfolane than in coordinating DMA, DMF, or DMSO (Table 2). Finally, ΔH values for formation of $\text{RCo}^{\text{III}}\text{Pc}(\text{L})$ in toluene and sulfolane are more negative than in coordinating solvents (Table 2), and the differences correspond, although very roughly, to ΔH for formation of DMA, DMF, or DMSO adducts with $\text{RCo}^{\text{III}}\text{Pc}$ in toluene.

Axial Ligation of $\text{RCo}^{\text{III}}\text{Pc}$. Data of Table 2 demonstrate that regardless of the solvent used, 4-NMe₂py and N-Melm are the most effective axial bases while pyridine and strongly basic piperidine are relatively weak binding ligands. When N-donors having the same pK_a of their protonated forms are compared, N-Melm seems to be a stronger binding, and piperidine a weaker binding ligand, than pyridines (Figure 5). The exceptional propensity of unhindered imidazoles for coordination to low-spin cobalt has been noted earlier and explained by a combination of strong σ -donor and π -acceptor properties.^{24,50} Differences in steric requirements will account for the observed order of ligational ability of N-donors of different structure but similar basicity equally well as π -bonding.⁵¹ The importance of steric effects for ligand coordination to the cobalt atom in rigid phthalocyanine is

evident from the low stability constant for the 2-Mepy adduct. Steric interactions are also responsible for relatively weak binding of aliphatic tertiary amines such as *N*-methylpiperidine and triethylamine (the latter not shown in Table 2 and Figure 5 because of lack of any detectable interaction). In contrast, less basic, and also less hindered, DABCO ($\text{pK}_a = 8.4$) belongs to the most effective ligands.

Comparison of the $\text{CH}_3\text{Co}^{\text{III}}\text{Pc}$ behavior to that of related $\text{CH}_3\text{Co}^{\text{III}}(\text{OEP})$ ⁴⁸ and $\text{Co}^{\text{II}}(\text{OEP})$ ⁵² is illuminating (Figure 5). A significant cis effect of the planar ligand is apparent from Figure 5. Due to stronger electron-donating properties of the porphyrin than the phthalocyanine system, Lewis acidity of $\text{CH}_3\text{Co}^{\text{III}}\text{Pc}$ in toluene is larger or comparable to that of tetracoordinate $\text{Co}^{\text{II}}(\text{OEP})$ ⁵⁶ despite the presence of a strong stabilizing axial ligand in the former. The response of stability constants to changes in σ -donor properties of isosteric substituted pyridines, measured by the slope of $\log K_L$ versus pK_a correlations seems to be a better yet gauge for the cis effect. The slopes of the straight lines shown in Figure 5 are 0.30 ± 0.03 , 0.10 ± 0.02 , and 0.08 ± 0.02 for $\text{CH}_3\text{Co}^{\text{III}}\text{Pc}$, $\text{CH}_3\text{Co}^{\text{III}}(\text{OEP})$, and $\text{Co}^{\text{II}}(\text{OEP})$, respectively. Interestingly, stability constants for $\text{CH}_3\text{Co}^{\text{III}}\text{Pc}(\text{L})$ show a very similar response to basicity of the nitrogenous ligands as possibly the most "electron poor" alkylcobalt model, $\text{CH}_3\text{Co}(\text{DH})_2(\text{L})$.^{46,53} Data of Ingraham et al.⁵⁷ for ligation of substituted pyridines by $\text{CH}_3\text{Co}(\text{DH})_2$ in 50% DMSO yield a slope of 0.28 ± 0.03 . Of note, the variance of stability constants for $\text{MeCbi}(4\text{-X-py})^+$ in hydroxylic solvents seems to be similar to that of $\text{CH}_3\text{Co}^{\text{III}}(\text{OEP})$ rather than $\text{CH}_3\text{Co}^{\text{III}}\text{Pc}$.⁵⁸

The demand of a Lewis acidic center in $\text{RCo}^{\text{III}}\text{Pc}$ for six-coordination can be compared to those of other alkylcobalt model compounds (R = primary alkyl group) when stability constants of adducts with nonbulky pyridine are considered. Unfortunately, even with this popular ligand, data for the same axial alkyl group in same solvent for a wide range of planar ligand systems are not accessible. Nevertheless, analysis of stability constants of Table 3 leads to a conclusion that $\text{CH}_3\text{Co}^{\text{III}}\text{Pc}(\text{py})$ complexes are less thermodynamically labile than other models, except alkylcobaloximes and Costa-type models. Methylcobaloxime exhibits a very strong demand for hexacoordination, indicated by large formation constants for pyridine adducts even in strongly coordinating DMSO (Table 3). Formation constants for $\text{RCo}^{\text{III}}(\text{saloph})(\text{py})$ have not been reported, but weakness of interaction can be concluded from the fact that some of these complexes

(49) Sirovatka-Dorweiler, J.; Matthews, R. G.; Finke, R. G. *Inorg. Chem.* **2002**, *41*, 6217.

(50) (a) Walker, F. A. *J. Am. Chem. Soc.* **1973**, *95*, 1150. (b) Terazono, Y.; Patrick, B. O.; Dolphin, D. H. *Inorg. Chim. Acta* **2003**, *346*, 265, and references therein.

(51) Jensen, F. R.; Kiskis, R. C. *J. Am. Chem. Soc.* **1975**, *97*, 5820.

(52) Summers, J. S.; Stolzenberg, A. M. *J. Am. Chem. Soc.* **1993**, *115*, 10559.

(53) Bresciani-Pahor, N.; Forcolin, M.; Marzilli, L. G.; Randaccio, L.; Summers, M. F.; Toscano, P. J. *Coord. Chem. Rev.* **1985**, *63*, 1.

(54) Parker, W. O., Jr.; Zagrando, E.; Bresciani-Pahor, N.; Marzilli, P. A.; Randaccio, L.; Marzilli, L. G. *Inorg. Chem.* **1988**, *27*, 2170.

(55) Samsel, E.; Kochi, J. *J. Am. Chem. Soc.* **1986**, *108*, 4790.

(56) Cobalt atom in the resultant five-coordinate $\text{Co}^{\text{II}}(\text{OEP})\text{L}$ complex can be pulled out of the plane only by some 0.1 Å. In $\text{CH}_3\text{Co}^{\text{III}}\text{Pc}(\text{L})$ and $\text{CH}_3\text{Co}^{\text{III}}(\text{OEP})(\text{L})$ species, cobalt lies exactly in the plane.

(57) Fox, J. P.; Banniger, R.; Proffitt, R. T.; Ingraham, L. L. *Inorg. Chem.* **1972**, *11*, 2379.

(58) Very limited data are available, no stability constant for a pyridine ligand with electron-withdrawing substituent is reported, and linear relationship between pK and pK_a has not been established (see ref 49).

Table 3. Formation Constants for Pyridine Binding by Alkylcobalt(III) Model Complexes

complex	solvent	temp (°C)	K_L (M^{-1})	ref
$\text{CH}_3\text{Co}^{\text{III}}(\text{DH})_2(\text{py})$	H_2O	25	2040	53
$\text{CH}_3\text{Co}^{\text{III}}(\text{DH})_2(\text{py})$	DMSO	32	910	53
$\text{CH}_3\text{Co}^{\text{III}}(\text{DO})(\text{DOH})\text{pn}(\text{py})^+$	DMSO	25	56	54
$\text{CH}_3\text{Co}^{\text{III}}\text{Pc}(\text{py})$	DMSO	25	5.9	this work
$\text{CH}_3\text{Co}^{\text{III}}\text{Pc}(\text{py})$	toluene	25	2410	this work
$\text{CH}_3\text{Co}^{\text{III}}\text{Pc}(\text{py})$	CH_2Cl_2	25	3630	this work
$\text{CH}_3\text{Co}^{\text{III}}(\text{OEP})(\text{py})$	toluene	20	57	48
$\text{CH}_3\text{Co}^{\text{III}}(\text{bae})(\text{py})$	CDCl_3	30	50	47a
$n\text{-BuCo}^{\text{III}}(\text{salen})(\text{py})$	CH_2Cl_2	22	22	55
$\text{CH}_3\text{Cbi}(\text{py})^+$	$\text{HOCH}_2\text{CH}_2\text{OH}$	25	6.1	49
$\text{CH}_3\text{Cbi}(\text{py})^+$	H_2O	25	6.9	49

(R = hexenyl) crystallize as a pentacoordinate form even from a 1:1 mixture of pyridine and CH_2Cl_2 .⁵⁵ No interaction with pyridine was detected in the case of $\text{RCo}^{\text{III}}(\text{tropocoronand})$ complexes.⁵⁹

Alternatively, acidity of alkylcobalt complexes has been characterized by kinetic lability of the trans axial ligand.^{60,61} The ease of ligand exchange has been linked to cis effects of the planar system, electron-rich systems being kinetically more labile. The exchange rates of py for PBu_3 in $\text{CH}_3\text{Co}^{\text{III}}\text{Pc}(\text{py})$ in toluene, and DMA for py or N-MeIm in $\text{CH}_3\text{Co}^{\text{III}}\text{Pc}(\text{DMA})$ in DMA, were too rapid for a stopped-flow measurement at ambient temperature. A temperature-jump attempt to measure the rates of dissociation of $\text{CH}_3\text{Co}^{\text{III}}\text{Pc}(\text{py})$ in 0.01–0.05 M py solutions in coordinating DMA yielded observed first-order rate constants on the order of $1 \times 10^4 \text{ s}^{-1}$ at 25 °C. The pyridine concentration dependence was weak. Larger py concentration range and higher accuracy would be needed for a detailed analysis in terms of reversible reaction with five-coordinate $\text{CH}_3\text{Co}^{\text{III}}\text{Pc}$ as an intermediate. In the absence of pyridine, a ~2-fold slower relaxation corresponding to temperature dependence of the $\text{CH}_3\text{Co}^{\text{III}}\text{Pc}$ spectra in DMA was observed. Anyway, this experiment, out of necessity performed in coordinating solvent,⁶² and the unsuccessful stopped-flow attempts to measure ligand exchange rates, show that ligand exchange in $\text{CH}_3\text{Co}^{\text{III}}\text{Pc}(\text{L})$ complexes is extremely fast compared to alkylcobaloxime⁶¹ or Costa-type⁶³ models.

In summary, both thermodynamic and kinetic evidence demonstrate that $\text{CH}_3\text{Co}^{\text{III}}\text{Pc}$ falls in the order of Lewis acidity of alkylcobalt complexes between MeCbi^+ or MeCbl and inert methylcobaloxime or Costa-type complexes. By electrochemical criteria, $\text{CH}_3\text{Co}^{\text{III}}\text{Pc}$ belongs to the most electron-deficient alkylcobalt(III) models.⁶⁴ Taking that into account, it should be noted that $\text{CH}_3\text{Co}^{\text{III}}\text{Pc}(\text{L})$ are relatively labile for electron-poor complexes. Possible reason for this

increased lability could be large unsaturated equatorial system⁶⁵ and steric bulk of the rigid phthalocyanine macrocycle.⁶⁶

Phosphines usually exhibit larger affinity for coordination to alkylcobaloximes than pyridine.^{53,67} Apparently, flexibility of the cobaloxime equatorial system facilitates coordination of bulky phosphine ligands.⁶⁸ With $\text{RCo}^{\text{III}}\text{Pc}$ complexes, tributylphosphine ($\text{p}K_a = 8.43$)⁵¹ is a considerably weaker binding ligand than pyridine ($\text{p}K_a = 5.17$). There is no spectral indication of any interaction of PPH_3 with alkylcobalt phthalocyanines even in noncoordinating toluene. This is in accordance with the observation that triphenylphosphine, due to its large cone angle, is a very poor ligand in related alkylcobalt(III) porphyrin complexes.⁶⁹

Poor affinity of O-donor ligands such as DMSO,⁷⁰ DMA, DMF, THF, and H_2O , for coordination to cobalt in $\text{RCo}^{\text{III}}\text{Pc}$ (Table 2) is consistent with similar behavior of other alkylcobalt complexes.^{61,71} The formation constant for $\text{CH}_3\text{Co}^{\text{III}}\text{Pc}(\text{DMA})$ in toluene is only 5.1 M^{-1} . Weakness of interaction is confirmed by $\Delta H = -3.8 \text{ kcal/mol}$. Since the σ -bonding ability of DMSO is considerably greater than that of amides such as DMF or DMA,⁷² the formation constant for $\text{CH}_3\text{Co}^{\text{III}}\text{Pc}(\text{DMSO})$ of 47.2 M^{-1} , i.e., substantially larger than for DMA complex, is not surprising at all.

It is plausible that the equilibrium constants for reactions that are not accompanied by charge separation, in the absence of solvent coordination, will not appreciably depend on solvent polarity.^{73,74} In this work, it is exemplified by similar values of stability constants in toluene and polar sulfolane (Table 2). Conditional stability constants, K_L , measured in coordinating solvents, should not be directly compared to those determined in the absence of solvent coordination. Hypothetical equilibrium constants, $K_L^{(5)}$, for ligation of five-coordinate $\text{RCo}^{\text{III}}\text{Pc}$ with L in coordinating solvent (Scheme 1), can be obtained according to eq 4. Stability constants, K_S , for $\text{RCo}^{\text{III}}\text{Pc}(\text{solvent})$ in coordinating solvents are not available, but when the values for ligation of DMA, DMF, or DMSO by $\text{RCo}^{\text{III}}\text{Pc}$ determined in toluene (Table 2) are used instead, then the calculated $K_L^{(5)}$ values (in coordinating solvents) are similar to those determined in toluene (Table 4). Hence, there is a reason to believe that,

(65) Hamza, S. A.; Dücker-Benfer, C.; van Eldik, R. *Inorg. Chem.* **2000**, *39*, 3777.

(66) Steric bulk of related porphyrin ligand has been underlined in: Chopra, M.; Hun, T. S. M.; Leung, W.-H.; Yu, N.-T. *Inorg. Chem.* **1995**, *34*, 5973.

(67) Schrauzer, G. N.; Windgassen, R. *J. Am. Chem. Soc.* **1966**, *88*, 3738.

(68) Cobaloximes and Costa-type complexes in general show great ability for binding of bulky ligands, which has been the reason for regarding them as B_{12} -anti-models: Doll, K. M.; Finke, R. G. *Inorg. Chem.* **2004**, *43*, 2611.

(69) Cao, Y.; Petersen, J. L.; Stolzenberg, A. M. *Inorg. Chim. Acta* **1997**, *263*, 139.

(70) Low formation constants for $\text{MeCoPc}(\text{SMe}_2)$ make the possibility that DMSO binds to $\text{RCo}^{\text{III}}\text{Pc}$ through S atom unlikely.

(71) Gushl, R. J.; Stewart, R. S.; Brown, T. L. *Inorg. Chem.* **1974**, *13*, 417.

(72) Orihashi, Y.; Nishikawa, M.; Ohno, H.; Tsuchida, E.; Matsuda, H.; Nakanishi, H.; Kato, M. *Bull. Chem. Soc. Jpn.* **1987**, *60*, 3731.

(73) Rillema, D. P.; Wicker, C. M. Jr.; Morgan, R. D.; Barringer, L. F.; Scism, L. A. *J. Am. Chem. Soc.* **1982**, *104*, 1276.

(74) Kadish, K. M.; Bottomley, L. A.; Beroiz, D. *Inorg. Chem.* **1978**, *17*, 1124.

(59) Jaynes, B. S.; Ren, T.; Masschelein, A.; Lippard, S. J. *J. Am. Chem. Soc.* **1993**, *115*, 5589.

(60) Costa, G.; Mestroni, G.; Cocevar, C. *Tetrahedron Lett.* **1971**, *21*, 1869.

(61) Gushl, R. J.; Brown, T. L. *Inorg. Chem.* **1973**, *12*, 2815.

(62) Requisite high concentration of $\text{RCo}^{\text{III}}\text{Pc}$ and cannot be attained in noncoordinating solvents.

(63) Marzilli, L. G.; Gerli, A.; Calafat, A. M. *Inorg. Chem.* **1992**, *31*, 4617 and references therein.

(64) Note also here that $\text{CH}_3\text{Co}^{\text{III}}\text{Pc}$ may serve as a model for a methylcorrinoid activated for nucleophilic attack at carbon.

Table 4. Calculated Equilibrium Constants, $K_L^{(5)}$, for Ligand Binding by Five-Coordinate $\text{RCo}^{\text{III}}\text{Pc}$ Species in Donor Solvents

$\text{RCo}^{\text{III}}\text{Pc}(\text{L})$	solvent	K_L^a	$K_L^{(5)b}$	$K_L^{(5)}/K_L^{(\text{Tot})c}$
$\text{CH}_3\text{Co}^{\text{III}}\text{Pc}(\text{py})$	DMA	42	2350	1.0
$\text{CH}_3\text{Co}^{\text{III}}\text{Pc}(\text{py})$	DMF	31	2750	1.1
$\text{CH}_3\text{Co}^{\text{III}}\text{Pc}(\text{py})$	DMSO	5.9	3930	1.6
$\text{CH}_3\text{Co}^{\text{III}}\text{Pc}(4\text{-NMe}_2\text{py})$	DMA	1840	103000	1.1
$\text{CH}_3\text{Co}^{\text{III}}\text{Pc}(\text{pip})$	DMA	710	39700	5.7
$\text{CH}_3\text{Co}^{\text{III}}\text{Pc}(\text{N-MeIm})$	DMA	2000	112000	2.0

^a Conditional equilibrium constants, M^{-1} , data from Table 2. ^b M^{-1} , calculated according to eq 4 as described in the text. ^c K_L in toluene (Table 2).

Table 5. ^1H NMR Data for $\text{CH}_3\text{Co}^{\text{III}}\text{Pc}(\text{X})$ Complexes^a in DMF-d_7

	phthalic protons ^b		CH_3^c
$\text{CH}_3\text{Co}^{\text{III}}\text{Pc}(\text{DMF-d}_7)$	9.49–9.51	8.26–8.29	−4.67 (15)
$\text{CH}_3\text{Co}^{\text{III}}\text{Pc}(\text{SCN})^{-d}$	9.46–9.49	8.23–8.26	−4.80 (1.8)
$\text{CH}_3\text{Co}^{\text{III}}\text{Pc}(\text{SeCN})^{-e}$	9.49–9.51	8.32–8.35	−4.72 (3.6)
$\text{CH}_3\text{Co}^{\text{III}}\text{Pc}(\text{CN})^{-}$	9.39–9.41	8.16–8.19	−5.10 (1.8)
$\text{CoPc}^{\text{III}}(\text{CN})_2^{-}$	9.54–9.56	8.30–8.33	

^a Ppm relative to TMS. ^b Multiplets, 8H each. ^c s, 3H, half-width, Hz, in parentheses. ^d 0.1 M KSCN. ^e 0.1 M KSeCN.

Table 6. Nitrogenous Axial Base Inhibition of Methyl Transfer from $\text{CH}_3\text{Co}^{\text{III}}\text{Pc}$ to Iodide in Dimethylacetamide (25 °C)

axial base (L)	[L] (M)	k_2^{app} ($10^{-3} \text{M}^{-1} \text{s}^{-1}$)	$K_L^{(\text{kin})a}$ (M^{-1})
pyridine	0–0.296	479–24.1	46 ± 9
N-MeIm	0–0.0609	479–3.91	1880 ± 60
N-MeIm ^b	0–0.821	4870–4.7	1100 ± 100
piperidine	0–0.0196	479–16.7	1370 ± 70
Et_3N	0–0.35	479–395	

^a Determined from the dependence of $1/k_2^{\text{app}}$ vs [L] (eq 8). ^b 45 °C, $K_L^{(\text{eq})} = 920 \pm 30 \text{M}^{-1}$.

at least for $\text{RCo}^{\text{III}}\text{Pc}$ complexes, K_S values in coordinating solvents can be reasonably approximated by formation constants determined in toluene. If, as argued above, the formation constant for $\text{CH}_3\text{Co}^{\text{III}}\text{Pc}(\text{DMA})$, determined in toluene, is indeed close to K_{DMA} in DMA, a few percent of the complex should persist as pentacoordinate species in DMA, and the percentage of the five-coordinate form would be 1 order of magnitude lower in DMSO. On the other hand, in sulfolane, which presents an interesting example of a very weakly coordinating polar solvent, the fraction of pentacoordinate $\text{RCo}^{\text{III}}\text{Pc}$ complexes must be much larger than in DMA.

Thiocyanate and Selenocyanate Reactions. Thiocyanate and selenocyanate reactions were studied in order to show that methyl transfer from $\text{CH}_3\text{Co}^{\text{III}}\text{Pc}$ to anionic nucleophiles has more general character and to explore possible axial base inhibition caused by those bidentate ions. Thiocyanate ion reacts with $\text{CH}_3\text{Co}^{\text{III}}\text{Pc}$ in DMA and sulfolane at ambient temperature very sluggishly yielding CH_3SCN and $\text{Co}^{\text{I}}\text{Pc}$ (see Experimental Section). In polar aprotic solvents nucleophilicity toward CH_3I decreases in the following order: $\text{I}^- \sim \text{Br}^- > \text{SCN}^-$.⁷⁵ Thus, substantially lower rates of thiocyanate reaction (Table 8) are consistent with $\text{S}_{\text{N}}2$ mechanism. In a slower yet process, $\text{CH}_3\text{CH}_2\text{Co}^{\text{III}}\text{Pc}$ gives

Table 7. N-Donor Inhibition of Methyl Transfer from $\text{CH}_3\text{Co}^{\text{III}}\text{Pc}$ to Thiocyanate in Dimethylacetamide and Sulfolane (60 °C)

solvent	$[\text{SCN}^-]$ (M)	[L] (M)	k_{obs} (10^{-3}s^{-1})	$K_L^{(\text{kin})a}$ (M^{-1})	$K_L^{(\text{eq})}$ (M^{-1})
Pyridine					
DMA	0.004	0–0.144	0.560–0.040	19 ± 2	19.5 ± 0.1
sulfolane	0.0077	0–0.192	0.771–0.027	350 ± 40	293 ± 7
N-MeIm					
DMA	0.004	0–0.02	0.560–0.051	500 ± 10	540 ± 10

^a Determined from the dependence of $1/k_{\text{obs}}$ vs [L], (eq 7).

Table 8. Solvent Effect on the Rates and Activation Parameters for Reactions of $\text{CH}_3\text{Co}^{\text{III}}\text{Pc}$ with Various Nucleophiles

solvent	k_2^a ($10^{-3} \text{M}^{-1} \text{s}^{-1}$)	ΔH^\ddagger (kcal/mol)	ΔS^\ddagger (cal mol ⁻¹ K ⁻¹)
$\text{CH}_3\text{Co}^{\text{III}}\text{Pc} + \text{I}^-$			
DMSO	1.51 ± 0.03	24.5 ± 0.3	10.8 ± 0.9
DMF	64 ± 2	24.8 ± 0.6	19 ± 2
DMA ^b	492 ± 5	19.7 ± 0.8	6 ± 3
sulfolane ^c	370 ± 20	18 ± 1	−1 ± 4
$\text{CH}_3\text{Co}^{\text{III}}\text{Pc} + \text{Br}^-$			
DMSO	0.215 ^d	24.9 ± 0.2	8 ± 1
DMF	5.9 ± 0.1	24.4 ± 0.2	13.0 ± 0.7
DMA ^b	68 ± 5	23.2 ± 1.2	14 ± 4
sulfolane ^c	64 ± 2	21.0 ± 0.5	7 ± 2
$\text{CH}_3\text{Co}^{\text{III}}\text{Pc} + \text{SCN}^-$			
DMA	1.60 ^e	24.0 ± 0.7	10 ± 2
sulfolane	4.67 ^e	22.5 ± 0.8	6 ± 2
$\text{CH}_3\text{Co}^{\text{III}}\text{Pc} + \text{PPh}_3$			
toluene	5.9 ± 0.2	13.1 ± 0.4	−25 ± 1
DMSO	0.24 ^f	nd	nd
DMA	0.48 ^f	nd	nd

^a 25 °C. ^b Reference 10. ^c Reference 14. ^d From temperature dependence 45–70 °C. ^e Extrapolated from temperature dependence 40–70 °C. ^f A rough value. From temperature dependence 50–70 °C.

$\text{CH}_3\text{CH}_2\text{SCN}$ and $\text{Co}^{\text{I}}\text{Pc}^-$ with evolution of marginal amounts of ethylene. Reaction products (see Experimental Section) and greater reactivity of methyl than ethylcobalt derivative is also entirely consistent with an $\text{S}_{\text{N}}2$ mechanism. The rates for thiocyanate reaction were measured over the temperature range 40–70 °C (see Table S5). Plots of k_{obs} versus $[\text{SCN}^-]$ show a marked negative curvature (Figures S9 and S10). A trivial reason for that, ion association of $\text{Bu}_4\text{N}^+\text{SCN}^-$ in the concentration ranges used, has been ruled out by conductivity. Kohlrausch plots for $\text{Bu}_4\text{N}^+\text{SCN}^-$ in both DMA and sulfolane are straight lines with theoretical slopes (see Experimental Section and Figure S12). The nonlinear dependence of k_{obs} can reasonably be ascribed to formation of inactive $\text{CH}_3\text{CoPc}(\text{SCN})^-$. While attack at carbon gives exclusively CH_3SCN (see Experimental Section), the cobalt atom in phtahlocyanine complexes has been shown to bind bidentate SCN^- ion either through S or N atom.⁷⁶ Therefore, the effective spectrophotometric formation constants of Table 2 may well refer to a mixture of $\text{CH}_3\text{CoPc}(\text{NCS})^-$ and $\text{CH}_3\text{CoPc}(\text{SCN})^-$. Chemical shift of phthalic protons in $\text{CoPc}(\text{SCN})_2^-$ is sensitive to the mode of SCN^- binding. In acetone- d_6 , three sets of phthalic signals have been observed indicating the presence of three isomers.⁷⁶ In contrast, the effect of 0.1 M SCN^- on ^1H NMR spectra of $\text{CH}_3\text{Co}^{\text{III}}\text{Pc}$ in

(75) Alexander, R.; Ko, E. C. F.; Parker, A. J.; Bronxton, T. J. *J. Am. Chem. Soc.* **1968**, *90*, 5049.

(76) Hedtmann-Rein, C.; Hanack, M.; Peters, K.; Peters, E. M.; Schnering, H. G. *Inorg. Chem.* **1987**, *26*, 2647.

DMF- d_7 is small; there is only one set of resonances slightly changed from those for $\text{CH}_3\text{Co}^{\text{III}}\text{Pc}$ (Table 5). The equilibrium is not entirely displaced to the right; thus, ligand exchange in $\text{CH}_3\text{Co}^{\text{III}}\text{Pc}(\text{SCN})^-$ must be fast on the NMR scale. The only perceptible change caused by the presence of thiocyanate is ~ 0.13 ppm upfield shift of the axial methyl signal with a considerable decrease in its half-width. The narrowed methyl proton signal may indicate formation of a well-defined six-coordinate complex.⁶⁹ With selenocyanate, the methyl resonance is broader and less shifted (Table 5) possibly due to lower yet than with SCN^- formation constant of selenocyanate adduct with $\text{CH}_3\text{Co}^{\text{III}}\text{Pc}$. The fact that the resonances of $\text{CH}_3\text{Co}^{\text{III}}\text{Pc}(\text{CN})^-$ coexist with those of $(\text{CH}_3\text{Co}^{\text{III}}\text{Pc}(\text{SeCN})^-)$, when KSeCN is contaminated with a small amount of cyanide, demonstrates that dissociation of CN^- from the former complex is slow.

Accuracy of the effective K_{SCN} values determined from kinetics (eq 6) is poor, since in the thiocyanate concentration ranges (< 0.01 M) k_{obs} was far from saturation, especially in DMA. The sense of using eq 6 was therefore to determine the second-order rate constants accurately, rather than K_{SCN} . Nevertheless, extrapolations from temperature dependencies of those effective K_{SCN} , listed in Table S5, give estimates for formation constants at 25 °C that roughly agree with the results of equilibrium studies given in Table 2. However, ligation of thiocyanate by $\text{CH}_3\text{Co}^{\text{III}}\text{Pc}$ is something of a problem, since in contrast to other ligands, the effective formation constants in both DMA and sulfolane seem to slightly increase with temperature and the reaction entropies are positive.

Selenocyanate is a much stronger nucleophile than thiocyanate.⁷⁵ Accordingly, it exhibits higher reactivity than thiocyanate; $\text{CH}_3\text{Co}^{\text{III}}\text{Pc}$ was demethylated by KSeCN (0.1 M) in DMF- d_7 in NMR probe with a half-life of ~ 40 min at 22 ± 2 °C. Traces of strongly binding, and deactivating,¹⁰ cyanide contaminant precluded detailed kinetic studies in dilute solutions.

Methyl Transfer to Phosphines. Reaction products with phosphines are consistent with $\text{S}_{\text{N}}2$ mechanism (see Experimental Section). A small amount of ethylene produced during the product identification assays of $\text{CH}_3\text{CH}_2\text{Co}^{\text{III}}\text{Pc}$ with PBu_3 and PPh_3 in DMA suggests that there is some, although not very significant, involvement of β -elimination. Tributylphosphine ligates by the organometallic substrate (Table 2). As observed earlier with anionic nucleophiles that coordinate to cobalt such as thiophenoxide¹¹ or cyanide¹⁰ saturation of k_{obs} versus $[\text{PBu}_3]$ occurs (eq 1, Figure 6). With nonbinding triphenylphosphine the plot of k_{obs} against $[\text{PPh}_3]$ is a straight line passing the origin (Figure 7). Whereas in toluene the reaction is clean, in polar aprotic solvents there is an unknown follow-up process at a rate comparable with that of methyl transfer. Details for the interested reader are available in Supporting Information. Rough results, listed in Table 8, show that the methyl transfer from $\text{CH}_3\text{Co}^{\text{III}}\text{Pc}$ to PPh_3 is slower in DMA and DMSO than in toluene.

Methyl Transfer to Amines. Weak amine bases such as pyridine do not demethylate $\text{CH}_3\text{Co}^{\text{III}}\text{Pc}$. At elevated temperatures, homolysis will occur instead of methyl transfer.²⁹

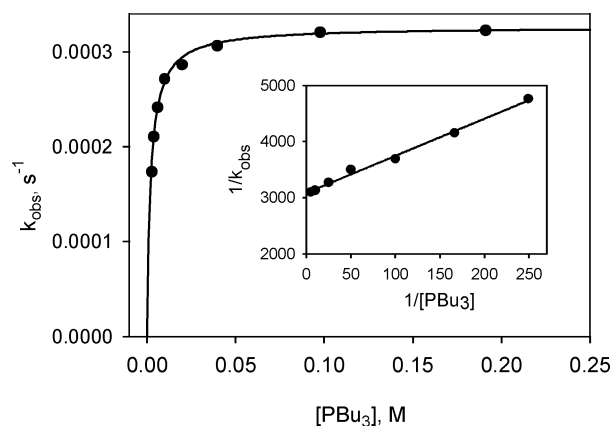


Figure 6. Saturation kinetics of methyl transfer from $\text{CH}_3\text{Co}^{\text{III}}\text{Pc}$ to PBu_3 in toluene (25 °C). The curve was calculated using $K_{\text{PBu}_3} = 460 \text{ M}^{-1}$ via eq 5 ($K_{\text{L}} = 0$). Inset: a double-reciprocal plot (eq 6). $[\text{CH}_3\text{Co}^{\text{III}}\text{Pc}] = (6\text{--}7) \times 10^{-6} \text{ M}$.

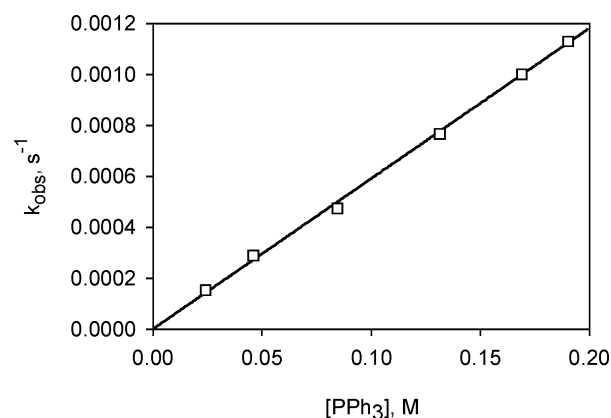


Figure 7. Concentration dependence of observed rate constant for the reaction of $\text{CH}_3\text{Co}^{\text{III}}\text{Pc}$ with PPh_3 in toluene (25 °C). $[\text{CH}_3\text{Co}^{\text{III}}\text{Pc}] = 7 \times 10^{-6} \text{ M}$.

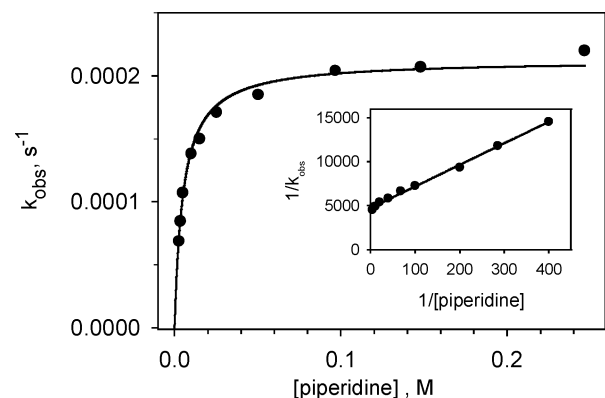


Figure 8. Rates for methyl transfer from $\text{CH}_3\text{Co}^{\text{III}}\text{Pc}$ to piperidine in DMA (60 °C). The curve was calculated via eq 5 ($K_{\text{L}} = 0$) using experimental stability constant $K_{\text{Nu}} = 200 \text{ M}^{-1}$. Inset: $1/k_{\text{obs}}$ versus $1/[\text{piperidine}]$ according to eq 6. $[\text{CH}_3\text{Co}^{\text{III}}\text{Pc}] = 9 \times 10^{-6} \text{ M}$.

In DMA at 60 °C, methyl transfer to aliphatic amines, albeit sluggish, is quantitative as indicated by product studies. Such quantitative methyl transfer from a methylcobalt(III) model to neutral amines is unprecedented. In analogy to phosphines, the concentration dependence of k_{obs} seems to depend on coordinating ability of an amine nucleophile. With coordinating piperidine saturation is observed (Figure 8) while in the case of noncoordinating Et_3N a plot resembling a straight

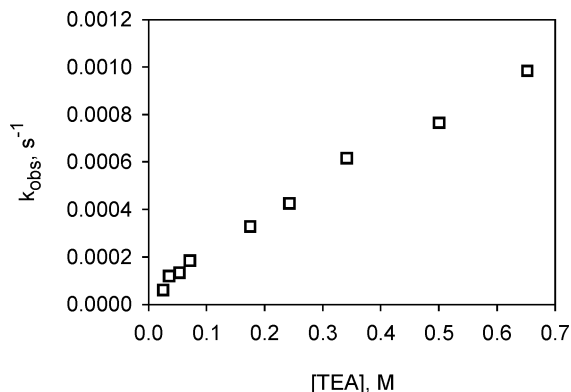


Figure 9. Rates for methyl transfer from $\text{CH}_3\text{Co}^{\text{III}}\text{Pc}$ to triethylamine in DMA (60 °C). $[\text{CH}_3\text{Co}^{\text{III}}\text{Pc}] = 8 \times 10^{-6}$ M.

line analogous to that of triphenylphosphine reaction rather than a saturation curve is obtained (Figure 9). A visible small negative curvature of this plot cannot be attributed to an interaction of Et_3N with the cobalt center, but coordination of a trace impurity or an axial base resulting from a side reaction of strongly basic NEt_3 with DMA solvent or its trace contaminants is very likely. Lack of saturation even at considerable ligand concentrations has been observed also for methyl transfer to weakly coordinating *N*-methylpiperidine (see Figure S16). Of note, at high concentrations of noncoordinating triethylamine nucleophile, the rates are larger than the saturated k_{obs} of piperidine reaction. The most straightforward and convincing explanation for very different behavior of coordinating and noncoordinating nucleophiles, whether anionic (I^- , no curvature; SCN^- , moderate curvature; PhS^- , CN^- saturation) or neutral (PPh_3 , no curvature, NEt_3 , *N*-Mepip, small curvature, PBu_3 and piperidine, saturation) that is born in one's mind is inactivity of six-coordinate $\text{CH}_3\text{-Co}^{\text{III}}\text{Pc}(\text{Nu})$ species. One might argue, and one of the reviewers actually has, that this behavior is consistent also with six-coordinate reactive species. However, at large concentrations of nonbinding nucleophiles such as PPh_3 or Et_3N , the fraction of $\text{CH}_3\text{Co}^{\text{III}}\text{Pc}(\text{Nu})$ is very small, yet the rates are similar or larger than the saturated rates measured with coordinating PBu_3 or piperidine nucleophiles. Moreover, *N*-MeIm inhibition of methyl transfer from $\text{CH}_3\text{Co}^{\text{III}}\text{Pc}$ to Et_3N appears to be very efficient (Figure S17). It would be hard to give a good reason why the PPh_3 and Et_3N adducts, i.e., complexes with virtually nonbinding nucleophiles, should be orders of magnitude more reactive than the PBu_3 , piperidine or *N*-methylimidazole adducts with $\text{CH}_3\text{Co}^{\text{III}}\text{Pc}$.

Nitrogenous Axial Base Inhibition of Methyl Transfer to Anionic Nucleophiles. To reduce experimental error, the effect of axial bases is best studied with nucleophiles that virtually do not coordinate to the cobalt center, such as iodide. The iodide reaction is also preferred because of fast rates. Axial bases such as pyridine, *N*-MeIm, and piperidine⁷⁷ and nonbinding triethylamine as a reference were used. The inhibition observed depended only on their ability to ligate the organometallic substrate. When $\text{RCo}^{\text{III}}\text{Pc}(\text{L})$ is completely inert, the apparent second-order rate constant $k_2^{\text{app}} = k_{\text{obs}}/$

(77) The rate of methyl transfer to piperidine can be neglected compared to the rate for iodide reaction.

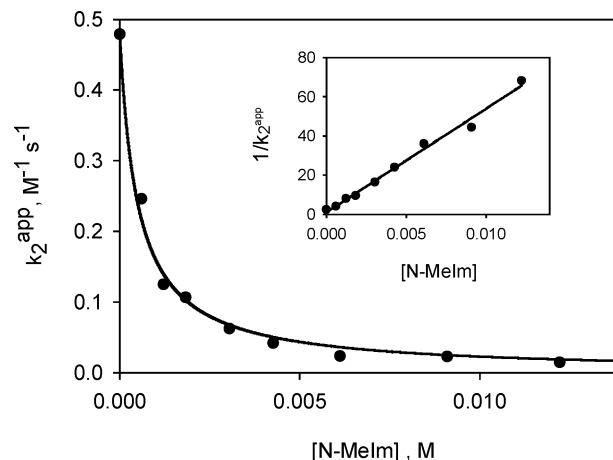


Figure 10. *N*-Methylimidazole inhibition of methyl transfer from $\text{CH}_3\text{-Co}^{\text{III}}\text{Pc}$ to iodide in DMA (25 °C). The curve was calculated for $K_L = 2000$ M⁻¹ (Table 2) and $k_2 = 0.48$ via eq 9. Inset: the plot of $1/k_2^{\text{app}}$ versus $[\text{N-MeIm}]$ (eq 8). $[\text{CH}_3\text{Co}^{\text{III}}\text{Pc}] = 9 \times 10^{-6}$ M.

$[\text{Nu}^-]$ for alkyl transfer will be given by eq 9. Strongly binding *N*-methylimidazole ligand is favorable, since extensive ligation can be achieved at low concentrations, thus making medium effects unimportant. As shown in Figure 10, experimental data fit the curve calculated via eq 9 well, so there is no need to take into account the reaction of $\text{CH}_3\text{-Co}^{\text{III}}\text{Pc}(\text{N-MeIm})$ species.

With weakly basic *N*-MeIm and pyridine, $K_L^{(\text{kin})}$ (Table 6) determined via eq 8 are not statistically different from the $K_L^{(\text{eq})}$ values resulting from equilibrium studies (Table 2). The concentration range, in which $\text{CH}_3\text{Co}^{\text{III}}\text{Pc}(\text{L})$ could compete with $\text{CH}_3\text{Co}^{\text{III}}\text{Pc}$, due to much larger concentration, has never been attained. For the *N*-MeIm inhibited iodide reaction in DMA at 45 °C, a 10³-fold rate decrease was observed with no perceptible deviation of the $1/k_2^{\text{app}}$ versus $[\text{N-MeIm}]$ plot from the straight line.

Piperidine inhibition proved even more effective than expected as indicated by $K_L^{(\text{kin})} \sim 2$ times larger than $K_L^{(\text{eq})}$. It is plausible that in the presence of strongly basic piperidine another axial base (not an *N*-donor though) is formed and the amount of the reactive five-coordinate species is lower than predicted from $K_{\text{pip}}^{(\text{eq})}$ alone. Virtually nonbinding Et_3N of similar basicity shows a weak inhibitory effect perhaps of the same origin (Table 6). *N*-donor inhibition of iodide reaction and also thiocyanate reaction (Table 7) is consistent with observations for methyl transfer to amines and phosphines and leads to a unified mechanism with unreactive six-coordinate methylcobalt(III) complexes.

Let us consider stabilization of the ground and transition state by a nitrogenous ligand. A substantial stabilization of the ground state (see large negative ΔH measured in toluene or sulfolane in Table 2) is, at least, largely lost in the $\text{S}_{\text{N}}2$ transition state due to negative charge developing on cobalt. Predissociation of $\text{CH}_3\text{Co}^{\text{III}}\text{Pc}(\text{L})$ offers an easier reaction path for methyl transfer because of large negative $T\Delta S$ (Table 2), which will partially compensate for unfavorable $-\Delta H$. Hence, reactivity of $\text{CH}_3\text{Co}^{\text{III}}\text{Pc}(\text{L})$ should not nearly match that of the five-coordinate species. Same conclusions pertain

to weakly binding oxygenous ligands, but the reactivity differential will be lower.

Solvent Effect on the Rates of Methyl Transfer. In Table 8, second-order rate constants for methyl transfer reactions and activation parameters are given. Nucleophiles that do not ligate the substrate, or weakly binding SCN^- and Br^- (in sulfolane), have been chosen. We will be looking for unusual effects resulting from differences in coordination ability of various solvents. Solvent effect on the rates of ordinary methyl transfer reactions in polar aprotic solvents, where there is no specific solvation of the substrates, will provide a reference point for subsequent semiquantitative considerations. Inspection of literature data leads to a conclusion that rates for a typical methyl transfer to iodide, bromide or thiocyanate should increase in the following order of solvents, $\text{DMSO} < \text{DMF} < \text{DMA}$, with rates in DMA up to 10-fold faster than in DMSO.⁷⁵ Data needed for a comparison of $\text{S}_{\text{N}}2$ reactivity in sulfolane to those in other polar aprotic solvents of interest are scarce. Rates for the reaction of N_3^- with *n*-BuBr decrease in the following order of solvents, $\text{DMA} > \text{DMF} > \text{DMSO} > \text{sulfolane}$,⁷⁸ the reaction in DMA being ~ 20 -fold faster than in sulfolane. Another example of $\text{S}_{\text{N}}2$ rates appreciably larger in DMA¹⁰ than in sulfolane⁷⁹ is the identity reaction of I^- with MeI with the ratio DMA/sulfolane of 9.1 at 25 °C. Consequently, it is to be expected that the rate of a methyl transfer proceeding by an $\text{S}_{\text{N}}2$ mechanism will be ~ 1 order of magnitude lower in sulfolane and DMSO than in DMA. The behavior of $\text{CH}_3\text{Co}^{\text{III}}\text{Pc}$ is not quite that expected for a typical methyl transfer. First, rates in sulfolane are comparable (iodide and bromide reaction) or slightly higher (thiocyanate reaction) in sulfolane than in DMA. The most plausible explanation seems to be deactivation of the substrate by solvent ligation to cobalt (eq 2), which is much more advanced in DMA than in sulfolane. Second, the rates in DMSO are 314 and 325 times smaller than in DMA for bromide and iodide reaction, respectively. This is well beyond the expected solvent effect. Here ligation of $\text{CH}_3\text{-Co}^{\text{III}}\text{Pc}$ by DMSO is considerably stronger than by DMA (Table 2), which combined with the “normal” $k^{\text{DMA}}/k^{\text{DMSO}}$ of ~ 10 will account for the observed solvent effect. Thus, weakly binding oxygenous ligands appear to be effective inhibitors of methyl transfer from cobalt.

Solvent Effect on Activation Parameters. The effect cannot be ascribed solely to differences in solvent coordination to cobalt since the usual slower rates for typical methyl transfer reactions in sulfolane and DMSO must be reflected in the ΔH^\ddagger and ΔS^\ddagger values. It is compelling, though, that ΔH^\ddagger for the reaction of $\text{CH}_3\text{Co}^{\text{III}}\text{Pc}$ with iodide, bromide, or thiocyanate is always the lowest in sulfolane, and transfer from DMA to sulfolane results in a ~ 2 kcal/mol decrease in ΔH^\ddagger , which is not much different from ΔH for dissociation of $\text{CH}_3\text{Co}^{\text{III}}\text{Pc}(\text{DMA})$ in toluene (Table 2). On transfer from DMA or DMF to sulfolane, a decrease in ΔS^\ddagger values is always observed in accord with stronger solvation of the

(78) Delpuech, J. J. *Tetrahedron Lett.* **1965**, 2111.

(79) Lewis, E. S.; McLaughlin, M. L.; Douglas, T. A. *J. Am. Chem. Soc.* **1985**, *107*, 6668; interpolated from rates at 15 and 35 °C.

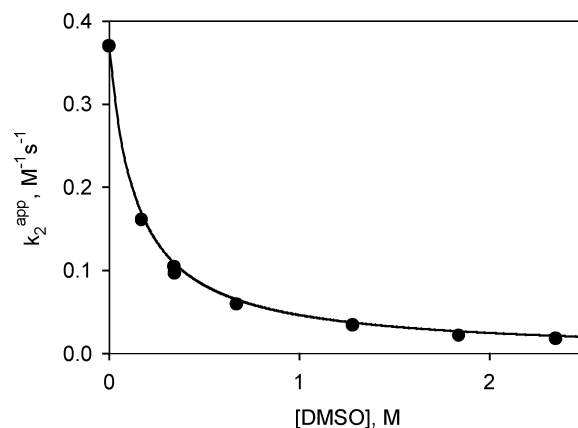


Figure 11. DMSO inhibition of iodide reaction of $\text{CH}_3\text{Co}^{\text{III}}\text{Pc}$ in sulfolane (25 °C). The curve was calculated for $K_{\text{DMSO}} = 6.3 \text{ M}^{-1}$ (Table 2) via eq 10, $k_{\text{L}} = 0$. $[\text{CH}_3\text{Co}^{\text{III}}\text{Pc}] = 7 \times 10^{-6} \text{ M}$.

ground state in the two binding solvents. Except for DMSO, the contributions resulting from coordination changes outweigh those caused by other solvation effects. The overall trends are consistent with the predissociation mechanism. Here, a question arises as to how to reconcile the postulated predominantly five-coordinate organometallic substrate in sulfolane with positive or only slightly negative ΔS^\ddagger values for methyl transfer in this solvent. Obviously, the predissociation argument does not apply to this case. It is conceivable, though, that ΔS^\ddagger values for the reaction of the pentacoordinate $\text{CH}_3\text{Co}^{\text{III}}\text{Pc}$ with anionic nucleophiles are inherently larger than “normal”⁸⁰ strongly negative values. Large negative $\Delta S^\ddagger = -25 \text{ cal mol}^{-1} \text{ K}^{-1}$ for the reaction of $\text{CH}_3\text{Co}^{\text{III}}\text{Pc}$ with PPh_3 in toluene can be accounted for by charge separation in the transition state.

Oxygenous Ligand Inhibition in Nondonor Solvents. With weakly binding O-donor ligands, a contribution from $\text{CH}_3\text{Co}^{\text{III}}\text{Pc}(\text{O-donor})$ to the overall methyl transfer rate cannot be a priori excluded. When medium effects are neglected, this leads, for a nonbinding nucleophile, to eq 10, where k_2^{app} is an apparent second-order rate constant (at

$$k_2^{\text{app}} = \frac{k}{K_{\text{L}}[\text{L}] + 1} + \frac{k_{\text{L}}K_{\text{L}}[\text{L}]}{K_{\text{L}}[\text{L}] + 1} \quad (10)$$

constant [L]) and k and k_{L} are second-order rate constants defined in Scheme 1. In the case of effective inhibition, $k_{\text{L}}K_{\text{L}}[\text{L}] \ll k$, the second term in eq 10 representing the reaction via the six-coordinate species disappears, i.e., a plot of k_2^{app} versus $1/(K_{\text{L}}[\text{L}] + 1)$, the fraction of ligand-free complex, should be a straight line yielding a slope k .

The reasoning, based on solvent effects on methyl transfer rates, leading to the conclusion that six-coordinate complexes are inactive is hinged on the assumption of predominantly five-coordinate $\text{CH}_3\text{Co}^{\text{III}}\text{Pc}$ species in sulfolane. If this conviction is justified, we should be able to observe O-donor ligand inhibition in this solvent. Effect of DMSO on the rates of iodide reaction in sulfolane is shown in Figure 11. Kinetic data fit the curve calculated using the stability constant for

(80) Lewis, E. S. *J. Am. Chem. Soc.* **1989**, *111*, 7576.

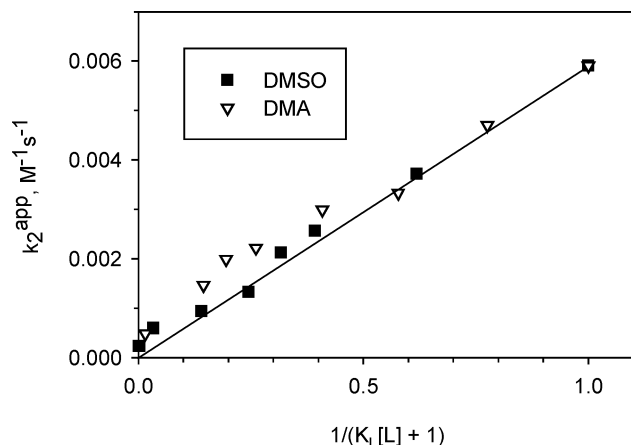


Figure 12. Oxygenous ligand ($L = \text{DMSO}$ or DMA) inhibition of the methyl transfer between $\text{CH}_3\text{Co}^{\text{III}}\text{Pc}$ and PPh_3 in toluene (25°C). The straight line was calculated for $k_L = 0$ according to eq 11. $[\text{CH}_3\text{Co}^{\text{III}}\text{Pc}] = 7 \times 10^{-6} \text{ M}$.

$\text{CH}_3\text{Co}^{\text{III}}\text{Pc}(\text{DMSO})$ in sulfolane⁸¹ (Table 2). The assumption of complete inertness of the hexacoordinate species works astonishingly well up to 1:1 DMSO in sulfolane. Moreover, the rate constant in DMSO calculated from k_2 in sulfolane (Table 8) and the stoichiometric concentration of DMSO in neat DMSO, using eq 10, $k_L = 0$, is $4.1 \times 10^{-3} \text{ M}^{-1} \text{ s}^{-1}$, i.e., larger merely by a factor of 2.7 than the experimental value. Deactivation of the organocobalt substrate by DMSO ligation is, clearly, the dominant factor. Thus, results of this experiment confirm the assumption of predominantly five-coordinate $\text{RCo}^{\text{III}}\text{Pc}$ in sulfolane. The second-order rate constants determined in this solvent, in the absence of axial bases added, should be referred to this complex.

Methyl transfer from $\text{CH}_3\text{Co}^{\text{III}}\text{Pc}$ to PPh_3 is slower in DMA or DMSO than in toluene (Table 8). This itself is an argument in favor of high reactivity of the five-coordinate species, for in polar solvents a stabilization of polar transition state is expected.⁸²

The reaction of $\text{CH}_3\text{Co}^{\text{III}}\text{Pc}$ with noncoordinating PPh_3 in toluene, where the organometallic substrate exists as five-coordinate species, seems to be well suited for studies of O-donor inhibition of methyl transfer from cobalt. In Figure 12, the apparent second-order rate constants for methyl transfer from $\text{CH}_3\text{Co}^{\text{III}}\text{Pc}$ to PPh_3 in toluene containing variable amounts of DMA or DMSO are plotted against $1/(K_L[L] + 1)$ (eq 10; K_L values of Table 2). The theoretical line for the case of completely inactive $\text{CH}_3\text{Co}^{\text{III}}\text{Pc}(L)$ is also shown. The data points for DMSO ligand, except for large [DMSO], fit the straight line while in the case of DMA inhibition, especially at larger ligand concentrations; they lie above the line. The deviation may be caused by a significant contribution from prevailing six-coordinate $\text{CH}_3\text{Co}^{\text{III}}\text{Pc}(\text{DMA})$ complexes to the overall methyl transfer rate (in contrast to the DMSO adduct) or by stabilization of polar transition state by DMA (note that considerably larger concentrations of DMA than DMSO are needed to achieve

the same value of $1/(K_L[L] + 1)$). The latter explanation is preferred in this work, especially since data points for small [DMA] fit the line. Hence, lower methyl transfer rates for PPh_3 reaction in DMSO and DMA than in toluene (Table 8) can be interpreted as a superposition of two inverse effects: prevailing oxygenous ligand inhibition and, secondary, stabilization of the transition state by polar solvents.

With very weak binding ligands such as DMA, kinetic competence of the five-coordinate species could not be rigorously demonstrated by an inhibition study similar to those described above, because large concentrations of the ligand significantly change properties of the solvent (and k in eq 10). In practice, the competence has to be inferred from solvent effects on the rates. The indirect evidence includes similar rates for the reactions in DMA and sulfolane (Table 8), as discussed above, and also, perhaps more convincing, the 10 times faster rates for PPh_3 reaction in toluene than in DMA. A 5 times larger k in polar DMA than in toluene would yield a good estimate of k_2^{app} for PPh_3 reaction in DMA via eq 10, $k_L = 0$.

Another argument for inactivity of the $\text{RCo}^{\text{III}}\text{Pc}(\text{DMA})$ species comes from analysis of eq 10. As the co-ligand interaction becomes increasingly weak, the narrowing gap in reactivity between the five- and six-coordinate species (increasing k_L) is accompanied by enhanced thermodynamic lability of the six-coordinate form (decreasing K_L). It seems reasonable that, in the absence of strong steric and medium effects, changes in O-donor strength will have larger impact on the equilibrium constant for the O-donor binding to cobalt than on methyl transfer reactivity of the $\text{CH}_3\text{Co}^{\text{III}}\text{Pc}(\text{O-donor})$ species. After all, in contrast to a nucleophile, the ligand binds directly to the acidic cobalt center. Consequently, with decreasing strength of the O-donor the $k_L K_L$ term in eq 10 should also decrease, and kinetic competence of the five-coordinate species demonstrated for one ligand could be automatically extended to all weaker ligands. Even though the above reasoning might be questioned, at least compensation would occur making changes in the $k_L K_L$ term slow. Since it has been demonstrated that with DMSO ligand $k \gg k_L K_L [L]$, and the difference in donor strength between DMSO and DMA is not dramatic, the kinetic competence of the five-coordinate species should hold also in the presence of very weak DMA ligand. It is tempting to generalize that the contribution from six coordinate $\text{CH}_3\text{Co}^{\text{III}}\text{Pc}(L)$ complexes to the overall methyl transfer rate can be neglected even if the six-coordinate form prevails in solution.

Alkyl Group Effect. Rates of Co(I) nucleophiles with alkyl halides conform to a profile characteristic of displacement reactions.⁸³ Ethyl derivatives are ~ 100 -fold slower than methyl compounds, and the same should be expected for dealkylations of the phthalocyanine complexes proceeding by an $\text{S}_{\text{N}}2$ mechanism. Except for the piperidine reaction, $\text{CH}_3\text{Co}^{\text{III}}\text{Pc}$ is always at least 1 order of magnitude more reactive than the ethyl derivative (Table 9), while the reverse is true for thermolysis.²⁹ This is entirely consistent with a displacement mechanism. The reactions of $\text{CH}_3\text{CH}_2\text{Co}^{\text{III}}\text{Pc}$

(81) In this case, the stability constant in toluene of 47 M^{-1} is significantly although not dramatically different than in sulfolane. Possibly DMSO is better stabilized by sulfolane than by toluene.

(82) Castejon, H.; Wiberg, K. B. *J. Am. Chem. Soc.* **1999**, *121*, 2139.

(83) Schrauzer, G. N.; Deutsch, E. *J. Am. Chem. Soc.* **1969**, *91*, 3341.

Table 9. Alkyl Group Effect on the Rates of $\text{RCo}^{\text{III}}\text{Pc}$ with Nucleophiles

nucleophile	solvent	temp (°C)	k_{Me} ($10^{-3}\text{M}^{-1}\text{s}^{-1}$)	K_{Me}^a (M^{-1})	k_{Et} ($10^{-3}\text{M}^{-1}\text{s}^{-1}$)	K_{Et}^a (M^{-1})	$k_{\text{Me}}/k_{\text{Et}}$
I^-	DMA	25	492 ^b		6.0 ± 0.2		82
Br^-	DMA	25	67.7 ^b		2.7 ± 0.1		25
SCN^-	DMA	60	240 ± 10	130 ± 50			9.1 ^c
PBU_3	toluene	25	150 ± 5^d	460 ± 20	2.9 ± 0.2^d	107 ± 9	52
PPh_3	toluene	25	5.9 ± 0.1		0.17 ± 0.02		35
piperidine	DMA	60	41 ± 5	200 ± 20^e			1.05 ^f
piperidine	toluene	60	$\sim 30^g$	860 ^h		244 ^h	0.25 ⁱ

^a Stability constants for $\text{RCoPc}(\text{nucleophile})$ determined from kinetic data (eq 6). ^b Data from ref 10. ^c A rough estimate: ratio of k_{obs} for dealkylation at $[\text{Bu}_4\text{NSCN}] = 0.008\text{M}$. ^d From a double-reciprocal plot. ^e Result of equilibrium measurements: 260 ± 20 . ^f Ratio of k_{obs} at $[\text{piperidine}] = 0.5\text{M}$ (saturation regime), $k_{\text{Me}} = 2.3 \times 10^{-4}\text{s}^{-1}$. ^g Saturated k_{obs} multiplied by K_{Me} . ^h From equilibria; an extrapolation from temperature dependence. ⁱ A ratio of k_{obs} at $[\text{piperidine}] = 0.25\text{M}$ (saturation regime); $k_{\text{Me}} = 3.5 \times 10^{-5}\text{s}^{-1}$.

with some nucleophiles are not clean, since a few percent of ethylene were detected in the product identification assays (see Experimental Section). Apart from concerted β -elimination, the ethylene may also be formed by homolytic fission of the $\text{Co}-\text{C}$ bond followed by hydrogen transfer.⁸⁴ With PBU_3 , taking into account low temperature at which the product identification assay was carried out, the former mechanism is more likely.

The $\text{S}_{\text{N}}2$ reactions of $\text{CH}_3\text{CH}_2\text{Co}^{\text{III}}\text{Pc}$ with weak nucleophiles proceed sluggishly, while homolysis of $\text{CH}_3\text{CH}_2\text{Co}^{\text{III}}\text{Pc}(\text{py})$ is faster than that of the methylcobalt complex.²⁹ As a result, especially at higher temperatures, the borderline region between $\text{S}_{\text{N}}2$ reactions and homolysis (vide $k_{\text{Me}}/k_{\text{Et}}$ ratios for piperidine reaction in Table 9) is approached. For that reason, and because of slow rates, kinetics of the reaction of $\text{CH}_3\text{CH}_2\text{Co}^{\text{III}}\text{Pc}$ with thiocyanate has not been studied in detail. Due to saturation-type dependence of k_{obs} on nucleophile concentration, a precise value for the second-order rate constant of methyl transfer from $\text{CH}_3\text{CH}_2\text{Co}^{\text{III}}\text{Pc}$ to thiocyanate has not been established, and the ratio of observed rate constants $k_{\text{obs}}^{\text{Me}}/k_{\text{obs}}^{\text{Et}}$ had to be taken in Table 9 as a rough estimate of relative reactivity of the two alkylcobalt complexes toward thiocyanate. This ratio is considerably lower than $k_{\text{Me}}/k_{\text{Et}}$ for I^- and Br^- nucleophiles. The ratio $k_{\text{Me}}/k_{\text{Et}}$ for the reaction of $\text{RCo}^{\text{III}}\text{Pc}$ with PBU_3 and PPh_3 in toluene is 52 and 35, respectively (Table 9), just what a displacement mechanism demands. Alkyl group effects, $k_{\text{Me}}/k_{\text{Et}}$ of 15–18 observed by Norris and Pratt⁵ for the reaction of alkylcobinamides with thiolates, including homocysteine, are not as large as some of those listed in Table 9, although still consistent with displacement mechanism. Small $k_{\text{Me}}/k_{\text{Et}}$ found by Hogenkamp et al.⁴ for dealkylations of alkylcobalamins by homocysteine are only seemingly the contrary of what is expected for $\text{S}_{\text{N}}2$ mechanism. Inactivity of the base-on form of RCbl must be taken into account. When rates for dealkylation of base-off form(s) of RCbl are calculated by employing equilibrium constants given by Brown and Peck-Siler,⁸⁵ then $k_{\text{Me}}/k_{\text{Et}} \sim 42$, i.e., characteristic of displacement reactions, is obtained (see Table S20). Thus, $\text{RCo}^{\text{III}}\text{Pc}$ model shares significant alkyl group effect, $\text{Me} > \text{Et}$, with alkylcorrinoids.

(84) Ng, F. T. T.; Remple, G. L.; Halpern, J. *J. Am. Chem. Soc.* **1982**, *104*, 621.

(85) Brown, K. L.; Peck-Siler, S. *J. Am. Chem. Soc.* **1988**, *27*, 3548.

Conclusions

Two factors, which cannot be rigorously separated, are crucial for methyl donor ability of a methyl cobalt(III) complex: electron-deficient character of the equatorial system and trans axial lability. With increasingly electron-poor properties of the complex, faster methyl transfer from the five-coordinate species is accompanied (and compensated) by stronger trans axial ligation. Due to steric factors, this compensatory effect is much stronger with methylcobaloxime than $\text{CH}_3\text{Co}^{\text{III}}\text{Pc}$.

In this work, axial base inhibition of methyl transfer from a methylcobalt(III) model has been demonstrated with variety of axial bases including thiocyanate ion, neutral N-donors, PBU_3 , and O-donors such as some polar aprotic solvents. When accurate values of equilibrium constants for ligation by $\text{CH}_3\text{Co}^{\text{III}}\text{Pc}$ are available, and medium effects can be neglected, the inhibition appears quantitative. This provides a reference point for methyl transfers from methylcorrinoids if only the properties of $\text{R}-\text{Co}-\text{L}$ axial system in $\text{CH}_3\text{Co}^{\text{III}}\text{Pc}(\text{L})$ are considered characteristic of methylcobalt(III) complexes. The $\text{MeCbi}/\text{MeCbl}$ rate ratios for thiolate reactions,⁵ which are larger than could be predicted from Brown's⁸⁵ base-on/off equilibrium constants for MeCbl , are an example of problems that need to be addressed.

Since the presence of a strong nitrogenous ligand accelerates homolytic cleavage of the $\text{Co}-\text{C}$ bond, and inactivates an alkylcobalt complex toward an $\text{S}_{\text{N}}2$ methyl transfer, the effect of axial ligation, best combined with alkyl group effect on the rate of dealkylation, allows an easy distinguishing between the two mechanisms.

Acknowledgment. Financial support from Polish State Committee for Scientific Research Grant 7 T09A 07421 is gratefully acknowledged.

Supporting Information Available: Figure S1, spectral changes on demethylation of $\text{CH}_3\text{Co}^{\text{III}}\text{Pc}$ by bromide in DMSO; Figure S2, spectral changes on pyridine addition to $\text{CH}_3\text{Co}^{\text{III}}\text{Pc}$ in CH_2Cl_2 ; thermochromism of $\text{CH}_3\text{Co}^{\text{III}}\text{Pc}$ (details); Figures S3–S7, diagnostic plots for $\text{CH}_3\text{Co}^{\text{III}}\text{Pc}$ ligation; Figure S8, van't Hoff plots for N-donor binding by $\text{CH}_3\text{Co}^{\text{III}}\text{Pc}$ in toluene; Figure S9, rates for the reaction of $\text{CH}_3\text{Co}^{\text{III}}\text{Pc}$ with SCN^- in DMA (40 °C); Figure S10, rates for the methyl transfer from $\text{CH}_3\text{Co}^{\text{III}}\text{Pc}$ to SCN^- in sulfolane (50 °C); Figure S11, Eyring plot for methyl transfer from $\text{CH}_3\text{Co}^{\text{III}}\text{Pc}$ to SCN^- in DMA; Figure S12, conductance of Bu_4NSCN in DMA and sulfolane (Kohlrusch plots); kinetics of the

reaction of $\text{CH}_3\text{Co}^{\text{III}}\text{Pc}$ with PPh_3 in toluene, and toluene containing DMA or DMSO (details); Figure S13, kinetic curves for the reaction of $\text{CH}_3\text{Co}^{\text{III}}\text{Pc}$ with triphenylphosphine in toluene and toluene containing DMA or DMSO; Figure S14, photolysis of the product of reaction of $\text{CH}_3\text{Co}^{\text{III}}\text{Pc}$ with PPh_3 in toluene in the presence of DMSO; Figure S15, effect of DMSO on the reaction spectra of $\text{CH}_3\text{Co}^{\text{III}}\text{Pc}$ with PPh_3 in toluene (25 °C); Figure S16, rates for the reaction of $\text{CH}_3\text{Co}^{\text{III}}\text{Pc}$ with *N*-methylpiperidine in DMA; Figure S17, *N*-MeIm inhibition of methyl transfer from $\text{CH}_3\text{Co}^{\text{III}}\text{Pc}$ to triethylamine; Figure S18, pyridine inhibition of methyl transfer from $\text{CH}_3\text{Co}^{\text{III}}\text{Pc}$ to SCN^- in sulfolane; Figures S19–S23, Eyring plots for methyl transfer from $\text{CH}_3\text{Co}^{\text{III}}\text{Pc}$ to halides in DMSO and DMF. Tables S1–S4, temperature dependencies of stability constants for $\text{CH}_3\text{Co}^{\text{III}}\text{Pc}$ (*N*-donor) complexes; Table S5, rates for the reaction of $\text{CH}_3\text{Co}^{\text{III}}\text{Pc}$ with thiocyanate; Tables S6–S8, rates for the reactions of $\text{CH}_3\text{Co}^{\text{III}}\text{Pc}$ and with $\text{CH}_3\text{CH}_2\text{Co}^{\text{III}}\text{Pc}$ phosphines in toluene; Table S9, rates for the reaction of $\text{CH}_3\text{Co}^{\text{III}}\text{Pc}$ with

piperidine in DMA; Table S10, rates for the reaction of $\text{CH}_3\text{Co}^{\text{III}}\text{Pc}$ with triethylamine in DMA; Table S11, rates for dealkylation of $\text{RCO}^{\text{III}}\text{Pc}$ in the presence of 0.25 M piperidine in toluene; Table S12, *N*-methylimidazole inhibition of methyl transfer from $\text{CH}_3\text{Co}^{\text{III}}\text{Pc}$ to iodide in DMA; Tables S13–S16, rates for methyl transfer from $\text{CH}_3\text{Co}^{\text{III}}\text{Pc}$ to halides in DMSO and DMF; Table S17, DMSO inhibition of methyl transfer from $\text{CH}_3\text{Co}^{\text{III}}\text{Pc}$ to iodide in sulfolane; Table S18, DMSO inhibition of methyl transfer from $\text{CH}_3\text{Co}^{\text{III}}\text{Pc}$ to PPh_3 in toluene; Table S19, DMA inhibition of methyl transfer from $\text{CH}_3\text{Co}^{\text{III}}\text{Pc}$ PPh_3 in toluene; Table S20, alkyl group effect on alkyl transfer from base-off alkylcobalamins to mercaptoethanol (recalculation). This material is available free of charge via the Internet at <http://pubs.acs.org>.

IC048698V